Stem Cell Reports
Article

ISSCR

OPEN ACCESS

Coupling between Myogenesis and Angiogenesis during Skeletal Muscle Regeneration Is Stimulated by Restorative Macrophages

Claire Latroche,[1,2] Michèle Weiss-Gayet,[3] Laurent Muller,[4] Cyril Gitiaux,[1] Pascal Leblanc,[3] Sophie Liot,[3] Sabrina Ben-Larbi,[3] Rana Abou-Khalil,[1] Nicolas Verger,[2] Paul Bardot,[1] Mélanie Magnan,[1] Fabrice Chrétien,[2] Rémi Mounier,[3] Stéphane Germain,[4] and Bénédicte Chazaud[1,3,*]

[1]Institut Cochin, INSERM U1016, CNRS UMR8104, Université Paris Descartes, PRES Sorbonne-Paris-Cité, 75014 Paris, France
[2]Institut Pasteur, Infection and Epidemiology Department, Histopathology and Animal Models Unit, 75015 Paris, France
[3]Institut NeuroMyoGène, Université Lyon, Université Claude Bernard Lyon 1, INSERM U1217, CNRS UMR5534, 16 rue Raphael Dubois, Bâtiment Gregor Mendel, 69100 Villeurbanne, France
[4]Collège de France, Center of Interdisciplinary Research in Biology, CNRS UMR7241, INSERM U1050, 75005 Paris, France
*Correspondence: benedicte.chazaud@inserm.fr
https://doi.org/10.1016/j.stemcr.2017.10.027

SUMMARY

In skeletal muscle, new functions for vessels have recently emerged beyond oxygen and nutrient supply, through the interactions that vascular cells establish with muscle stem cells. Here, we demonstrate in human and mouse that endothelial cells (ECs) and myogenic progenitor cells (MPCs) interacted together to couple myogenesis and angiogenesis *in vitro* and *in vivo* during skeletal muscle regeneration. Kinetics of gene expression of ECs and MPCs sorted at different time points of regeneration identified three effectors secreted by both ECs and MPCs. Apelin, Oncostatin M, and Periostin were shown to control myogenesis/angiogenesis coupling *in vitro* and to be required for myogenesis and vessel formation during muscle regeneration *in vivo*. Furthermore, restorative macrophages, which have been previously shown to support myogenesis *in vivo*, were shown in a 3D triculture model to stimulate myogenesis/angiogenesis coupling, notably through Oncostatin M production. Our data demonstrate that restorative macrophages orchestrate muscle regeneration by controlling myogenesis/angiogenesis coupling.

INTRODUCTION

Skeletal muscle is highly vascularized and myofibers are laced with a dense microvasculature. Numerous studies have reported the importance of vascularization in skeletal muscle function as well as the plasticity of vessels to adapt to the physiological demand (Latroche et al., 2015a). The organization of the vascular bed in adult skeletal muscle is well understood, and a microvascular unit was described to comprise 5–10 capillaries located in between 3 and 4 adjacent myofibers (Gitiaux et al., 2013; Latroche et al., 2015a). This vascular organization is altered in muscle diseases characterized by an important muscle regeneration process, including those directly affecting the vessels (Gitiaux et al., 2013, 2016) or the myofibers (Latroche et al., 2015b). Muscle regeneration relies on the capacities of satellite cells (SCs), the muscle stem cells, to activate and proliferate, giving rise to a population of transient amplifying myogenic precursor cells (MPCs) that express Pax7 and then the transcription factors Myf5 and MyoD (Yin et al., 2013). Later on, MPCs exit the cell cycle, enter into terminal myogenic differentiation, and fuse to form new myofibers. A subset of MPCs does not differentiate and self-renews to replenish the SC pool (Yin et al., 2013). Numerous studies have shown that the close microenvironment of SCs and MPCs is crucial for good implementation of adult myogenesis and skeletal muscle regeneration, including immune cells, notably macrophages (Arnold et al., 2007; Saclier et al., 2013), and fibro-adipogenic precursor (FAPs) cells (Joe et al., 2010; Uezumi et al., 2010).

Studies have demonstrated the importance of the interactions between the vessels and myogenic cells, besides the supply of oxygen and nutriments. *In vivo*, myonuclei (Ralston et al., 2006) and SCs (Christov et al., 2007) are preferentially associated with vessels along the myofiber. In resting conditions, the number of capillaries surrounding a myofiber is highly correlated with the number of SCs associated with the same myofiber (Christov et al., 2007). Specific subsets of peri-ECs exhibit some potent myogenic properties (Pannerec et al., 2012) while other peri-ECs are involved in the maintenance of the quiescence of SCs (Abou-Khalil et al., 2009). During muscle regeneration, the vascular bed undergoes profound alterations, with increased number of capillaries, branching, and anastomosis (Hardy et al., 2016), associated with the activation of endothelial cells (ECs) (Hansen-Smith et al., 1996). ECs and SCs concomitantly proliferate after an injury *in vivo* (Roberts and McGeachie, 1990) and the two cell types cooperate *in vitro*. ECs stimulate MPC growth while MPCs exhibit angiogenic-like properties (Christov et al., 2007; Germani et al., 2003; Rhoads et al., 2009). A series of growth factors were involved in these interactions, including vascular endothelial growth factor (VEGF), insulin growth factor (IGF) 1, platelet-derived growth factor (PDGF)-BB, hepatocyte growth factor (HGF), and basic

fibroblast growth factor (bFGF) (Arsic et al., 2004; Borselli et al., 2010; Bryan et al., 2008; Christov et al., 2007).

While these studies show privileged interactions between ECs and MPCs in regenerating muscle, the impact of ECs on myogenesis and that of SCs/MPCs on vessels, as well as the underlying molecular mechanisms, is still not documented. Here, we aimed to demonstrate the spatiotemporal cellular coupling of myogenesis and angiogenesis during muscle regeneration by using various human cell coculture systems and an *in vivo* angiogenesis assay. We further investigated the molecular effectors at work by performing high-throughput kinetic analyses of genes expressed by ECs and SCs during skeletal muscle regeneration. Functional experiments identified three molecular regulators of myogenesis/angiogenesis coupling that are required for a proper skeletal muscle regeneration. Finally, we investigated the role of anti-inflammatory, or restorative, macrophages, which are present in regenerating muscle, at the time when myogenic differentiation and angiogenesis take place, by establishing a 3D triculture setup mimicking the complex cellular crosstalks at work during skeletal muscle regeneration.

RESULTS

ECs Stimulate *In Vitro* Myogenesis

Interactions between MPCs and ECs were investigated using primary human cells. Using a bicameral chemotaxis assay (Figure 1A1), we showed that ECs enhanced the mean MPC migration distance by 29% (Figure 1A1), as well as the number of migrating MPCs (+220%, not shown), therefore greatly enhancing the migrating distance of the whole MPC population (+306%) (Figure 1A2). EC-conditioned medium increased MPC proliferation by 64% (Figure 1B), and even more their myogenin expression (+95%), indicating their entry into terminal myogenesis (Figure 1C). Under these conditions, i.e., very low serum-containing medium, EC-conditioned medium had no impact on fusion of already differentiated myocytes (mononucleated myogenin expressing cells) (Figure 1D). Thus, ECs exhibited pro-myogenic properties by stimulating MPC migration, proliferation, and their terminal differentiation.

MPCs Promote *In Vitro* Angiogenesis

MPCs enhanced mean EC migration by 30% (Figure 2A1), as well as the number of migrating ECs (+165%, not shown), therefore greatly enhancing the migration distance of the whole EC population (+200%) (Figure 2A2). MPC-conditioned medium had no effect on EC proliferation (Figure 2B). MPC angiogenic properties were investigated using a 3D angiogenic model that recapitulates the key stages of angiogenesis until the formation of an intraluminal compartment enabling the assessment of the full differentiation of the capillary structures that are formed (Nakatsu and Hughes, 2008). ECs seeded alone formed poorly developed capillaries (Figure 2C, none). Thus, human dermal fibroblasts were layered on top of the gel as a positive control (Ferratge et al., 2017). MPCs deposited on top of the gel (MPC ON in Figure 2C) exhibited a similar pro-angiogenic activity. When MPCs were seeded within the gel, the formation of capillaries was significantly stimulated in a dose-dependent way (MPC IN 50-100-250, Figure 2C1). Moreover, the presence of MPCs within the gel strongly increased the number of lumenized capillaries (Figure 2C2), indicative of a positive effect of MPCs on vessel maturation. The presence of myotubes was observed when MPCs were cocultured within the gel (arrows, Figure 2C) indicative of concomitant myogenesis and angiogenesis. Moreover, testing undifferentiated MPCs, differentiated mononucleated cells (myocytes), and fully differentiated multinucleated cells (myotubes) showed that the more myogenic cells were differentiated, the more they stimulated capillary elongation (Figure 2D1) and lumenization (Figure 2D2), highlighting a tight coordination between myogenesis and angiogenesis.

MPCs Promote *In Vivo* Angiogenesis

In vivo angiogenic properties of MPCs were evaluated using the Matrigel plug assay, in which the development of capillary blood vessels from the host inside the plug correlates with the angiogenic property of molecules initially embedded into the plug (Ito et al., 1996). The number of vessels ($CD31^{pos}$ structures) (Figures 3A and 3B) detected in the plug was greatly increased (+755%) when MPCs were embedded into the plug, compared with plugs embedded with fibroblasts or containing no cells (Figure 3C). The $CD31^{pos}$ structures formed functional capillaries since the hemoglobin content of the plug was increased by 93% in the presence of MPCs (Figure 3D). Accordingly, these vessels appeared well differentiated as they were surrounded by α-smooth muscle actin (SMA)-expressing cells, evocative of perivascular cells (Figure 3E). The high positive correlation observed between the presence of $desmin^{pos}$ cells (myotubes) and of $CD31^{pos}$ cells (vessels) (Figure 3F) confirmed the *in vitro* data and showed that myogenesis and angiogenesis are also coupled *in vivo*.

Molecular Analysis of Myogenesis/Angiogenesis Coupling

Microarray analysis of ECs and MPCs sorted at different time points (days 0, 2, 4, 8, after cardiotoxin injury) during muscle regeneration in mouse was performed. Purity of sorted cells was checked by immunocytochemistry

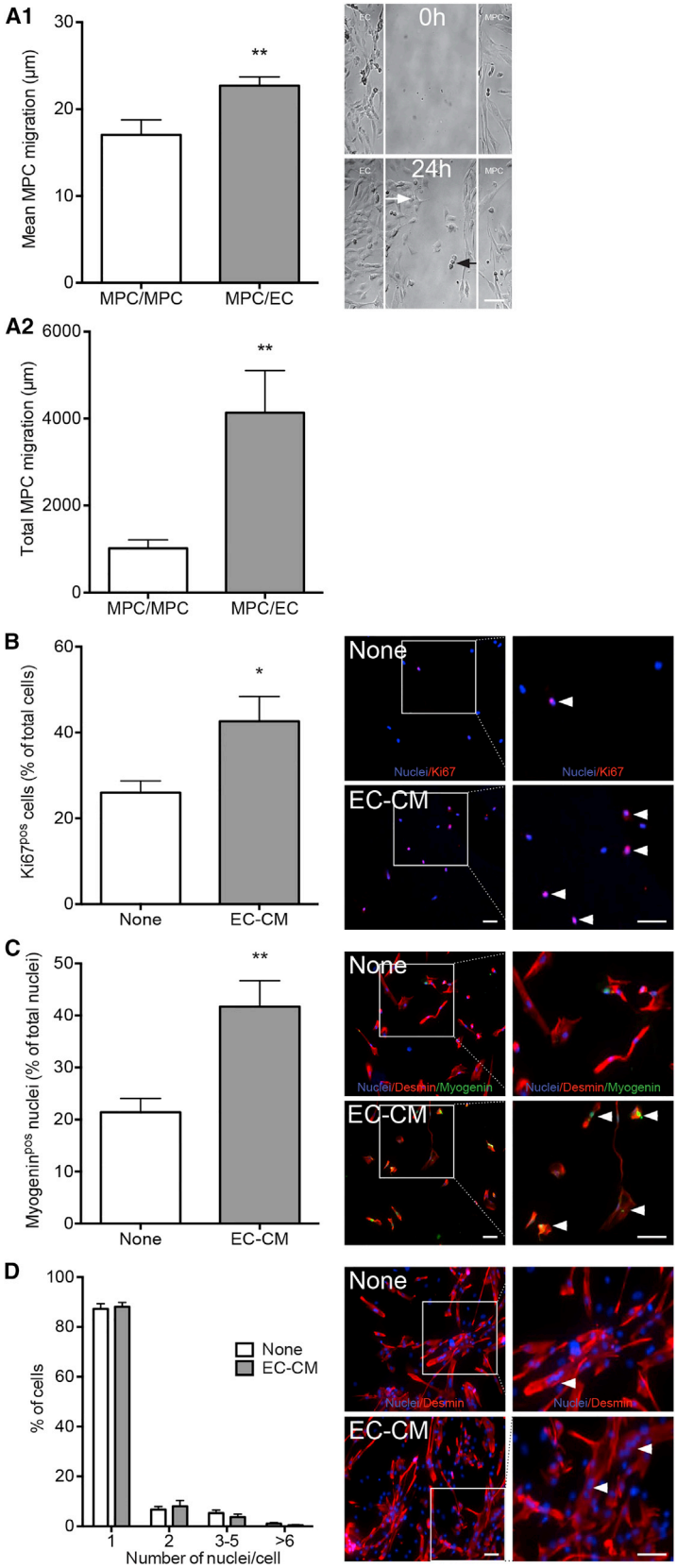

Figure 1. Pro-myogenic Properties of ECs

(A) MPCs and ECs were seeded in two separate chambers whose walls were removed 12 hr later so that the two cell types faced each other, allowing migration toward each other over a 24 hr period. Black and white arrows indicate the migrating distance of an MPC and an EC, respectively. (A1) Mean individual MPC migration distance toward ECs (MPC/EC), (A2) total migration distance of the migrating MPCs. Control included migration of MPCs toward MPCs (MPC/MPC).

(B and C) MPCs were cultured at low density with (EC-CM) or without (none) EC-conditioned medium. (B) Proliferating MPCs were counted as $Ki67^{pos}$ cells (red, arrowheads). (C) Differentiating MPCs were counted as $myogenin^{pos}$ (green, arrowheads) nuclei among $desmin^{pos}$ cells.

(D) Myocytes were cultured at high density with or without EC-CM. Myotubes ($desmin^{pos}$, red, arrowheads) were counted according to their number of nuclei.

Results are means ±SEM of six independent experiments. Bars, 50 µm. Blue, Hoechst. Mann-Whitney test was performed versus MPC/MPC (A), or none (C and D): *$p < 0.05$, **$p < 0.01$.

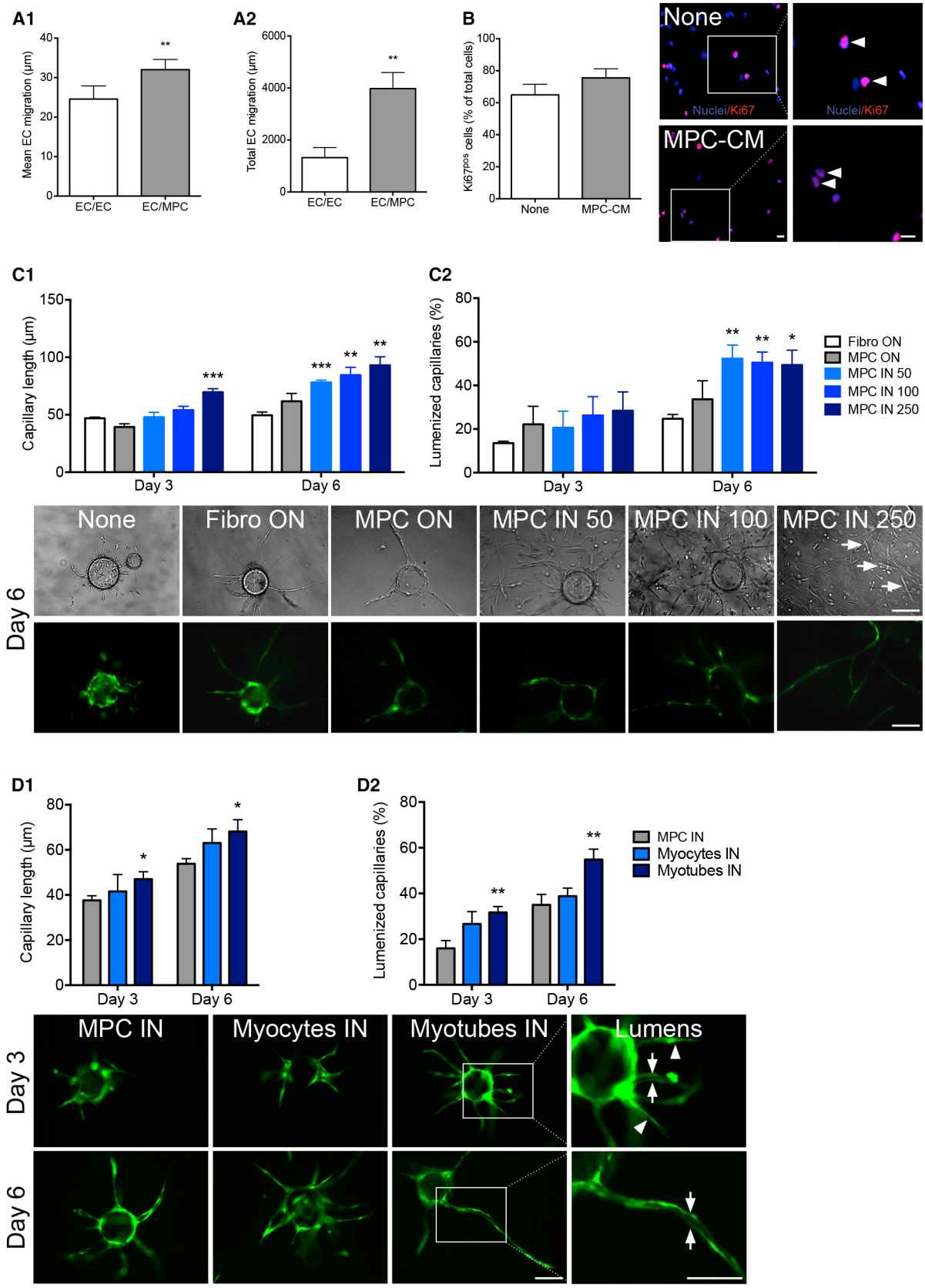

(legend on next page)

performed on cytospin preparations (Figures S1A–S1I). A total of 2,725 and 1,715 genes were significantly up- or downregulated in SCs and ECs, respectively, during muscle regeneration. For each cell type, differentially expressed genes were gathered into clusters according to their kinetics of expression (Figure S2). Enrichment in gene ontologies (GOs) (cell process) was calculated for each cluster using DAVID software. SC clusters enriched for GOs related to angiogenesis (i.e., clusters 1 and 5 in Figure S2A) and EC clusters enriched for myogenesis (i.e., clusters 2, 4, 5, 7 in Figure S2B) were selected. Using Pathway Studio software, extracellular molecules present in these clusters were analyzed for their capacity to enhance angiogenesis or myogenesis enrichment in the gene clusters expressed by the other cell type (see strategy in Figure S1). The screening gave rise to a series of molecules among which those expressed by both ECs and MPCs were selected (Table S1). Most of these molecules were already shown to regulate myogenesis and angiogenesis, separately (e.g., *Ace*, *Adam12*, *Angpt2*, *Dcn*, *Efnb1*, *Il1b*, *Il6*, *Lgals1*, *Sparc*,…) or concomitantly during muscle regeneration (e.g., *Ccl2*, *Igf1*, *Spp1*) (Table S1). Among the genes expressed by both ECs and MPCs during muscle regeneration that have not been deeply investigated and for which inhibitory tools were available, *Apln* (Apelin), *Postn* (Periostin), and *Osm* (Oncostatin M) were identified. Apelin (APLN) acts through APJ receptor, a G protein-coupled receptor, and is involved in angiogenesis. Oncostatin M is a member of the gp130/IL-6 cytokine family and exerts pleiotropic effects through OSM receptor (OSMR) in mouse and OSMR and leukemia inhibitory factor receptor in human. First identified in bone, Periostin (POSTN) seems to play an essential role in tissue remodeling in response to injury. *Apln*, *Postn*, and *Osm* showed differential profile expression during muscle regeneration, with a peak of expression at day 2 for *Apln* and *Osm* and a peak at day 4–8 for *Postn* (Figure S3A). Their cognate receptors were also expressed (except for POSTN, which interacts with multiple cell-surface receptors, including αvβ3-and αvβ5-integrins, therefore activating several pathways involved in cell adhesion and migration [Butcher et al., 2007]). Expression of the molecules and their receptors was confirmed by RT-qPCR in growing human MPCs and ECs *in vitro* (Figure S3B).

Apelin, Oncostatin M, and Periostin Stimulate *In Vitro* Myogenesis and *In Vivo* Angiogenesis

Recombinant proteins were added to MPCs in a medium containing 5% fetal bovine serum (FBS) to mimic a complex microenvironment. Figure 4A shows that APLN stimulated MPC proliferation in a dose-dependent way (up to 112%, Figure 4A1) and their differentiation into myocytes (up to 121%, Figure 4B1). Moreover, it stimulated the fusion of differentiated myocytes (up to 78%, Figure 4C1). Similar results were obtained with OSM, which was shown, for some concentrations, to stimulate the three steps of *in vitro* myogenesis (up to 187, 141, and 98%, respectively; Figures 4A2, 4B2, and 4C2). POSTN did not affect MPC proliferation (Figure 4A3), but it promoted their differentiation (63%, Figure 4B3) and myocyte fusion into myotubes (55%, Figure 4C3) in a dose-dependent manner, in accordance with the later expression of *Postn* during skeletal muscle regeneration (Figure S3). These results indicate that APLN, OSM, and POSTN support myogenesis.

Figure 4D shows that the presence of APLN, OSM, or POSTN strongly supported the development of blood vessels in the Matrigel plug assay (+196%, +230%, and 58%, respectively).

Apelin, Oncostatin M, and Periostin Directly Control Myogenesis/Angiogenesis Coupling

A 3D angiogenesis assay (using GFP-ECs) was used with red fluorescent protein (RFP)-labeled MPCs to analyze

Figure 2. Pro-angiogenic Properties of MPCs

(A) MPCs and ECs were cultured as described in Figure 1A1. (A1) Mean individual cell migration and (A2) total migration distance of ECs toward MPCs (EC/MPC) were measured. Control included migration of ECs toward ECs (EC/EC).

(B) ECs were cultured with (MPC-CM) or without (none) MPC-conditioned medium. Proliferating ECs were counted as $Ki67^{pos}$ cells (red, arrowheads) (blue, Hoechst).

(C and D) 3D capillary formation assay. (C) Cytodex beads coated with GFP-ECs were seeded in 3D fibrin gels alone (none) or with fibroblasts on top of the gel (Fibro ON), MPCs on top (MPC ON), or inside (MPC IN) the gel at different concentrations (50,000, 100,000, or 250,000 cells/mL). Capillary length (C1) and lumenization (C2) were measured after 3 and 6 days of culture. Pictures show representative examples of beads at day 6 on phase contrast (upper panel) and fluorescence (lower panel) of the same field. Myotubes are indicated by white arrows. (D) A 3D angiogenesis assay was performed using undifferentiated myoblasts (MPCs), myocytes, or multinucleated myotubes seeded in the gel (100,000 cells/mL) and capillary length (D1) and lumenization (D2) were estimated. Pictures show representative examples of beads at days 3 and 6. Magnifications on the right show capillaries with lumen (arrows) and without lumen (arrowheads). MPC IN 100 triggered different effects on capillary length in C1 and D1 (but similar effects on lumenization in C2 and D2) likely due to different human primary cultures.

Mann-Whitney test was performed versus EC/EC (A), none (B), fibroblasts (C), and MPCs (D): *$p < 0.05$; **$p < 0.01$; ***$p < 0.001$. Results are means ± SEM of six (A), five (B), five (C), and three (D) independent experiments. Bars, 100 μm.

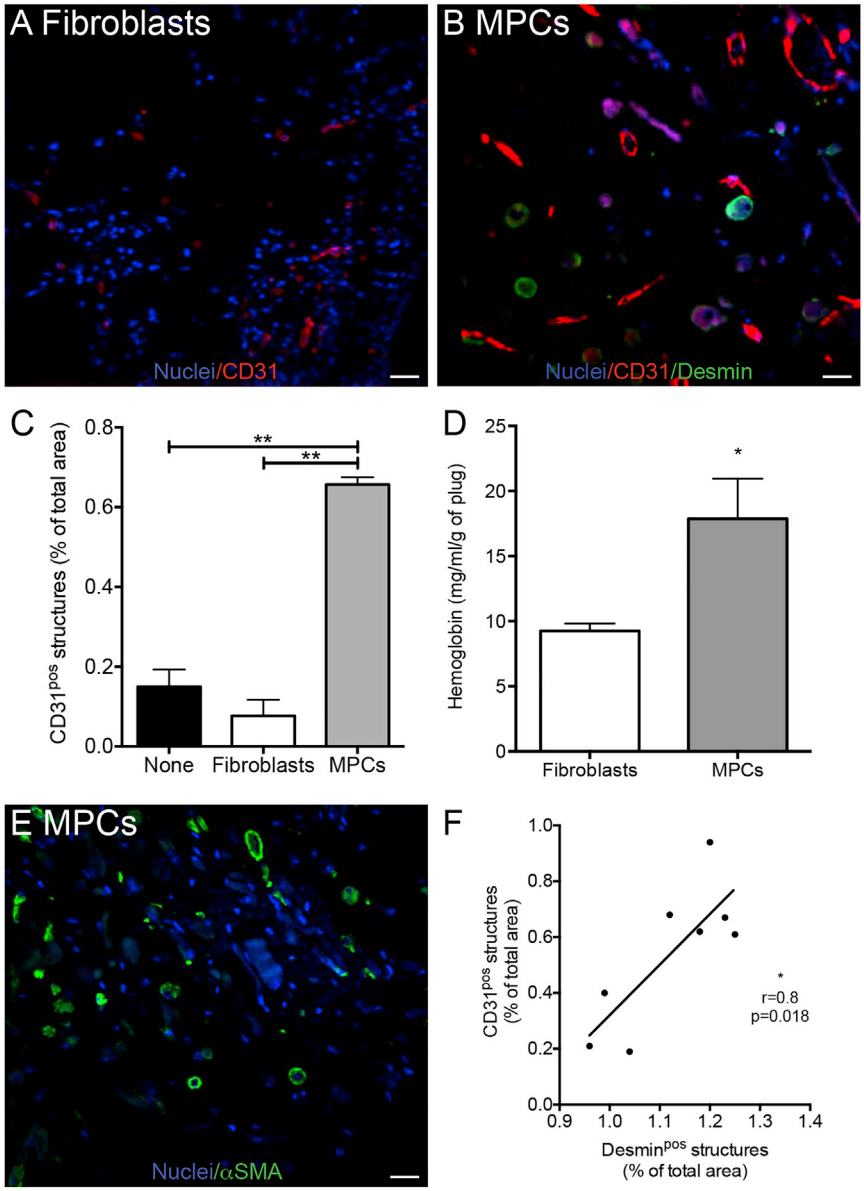

Figure 3. MPC Angiogenic Activity *In Vivo*

(A–D) Matrigel plugs containing no cells (none), fibroblasts, or MPCs were injected subcutaneously into mice and were excised 3 weeks later. Representative pictures of plugs containing fibroblasts (A) or MPCs (B) stained for CD31 (red) and for desmin (green). Quantification of the presence of $CD31^{pos}$ structures (C) and hemoglobin content (D) in the plug.

(E) Representative picture of a plug containing MPCs stained for α-smooth muscle actin (SMA) (green).

(F) Correlation of the number of $CD31^{pos}$ (endothelium) and $desmin^{pos}$ (myogenic) structures.

Blue, Hoechst.

Results are means ± SEM of five independent experiments. Mann-Whitney test was performed versus MPCs (C) or fibroblasts (D): *p < 0.05; **p < 0.01. Bars, 50 μm.

myotube formation. We compared the formation of capillaries and myotubes in the absence of MPCs and ECs, respectively. ECs cultured alone formed short capillaries with no lumen while the presence of MPCs strongly increased both processes (Figures 5A and 5C). Inversely, while MPCs were capable of fusion when cultured alone in the 3D gel, the presence of ECs strongly increased myotube formation (+180%) (Figure 5E), confirming the reciprocal stimulation of the two cell types. Blocking either APLN, OSM, or POSTN (antibodies/inhibitors were added within the gel) strongly inhibited capillary morphogenesis, including capillary elongation (−10%, −15%, −22%, respectively) (Figures 5A and 5B) and lumenization (−36%, −39%, −38%, respectively) (Figures 5C and 5D), as well as myotube formation (−59%, −49%, −74%, respectively) (Figures 5E and 5F). Blocking antibodies did not fully blunt the stimulated angiogenesis and myogenesis, suggesting that other factors are involved. Adding IgGs or the blocking antibodies to ECs cultured alone did not affect the weak capillary formation, indicating a specific effect of these molecules on MPC-driven capillarization and lumenization (Figures 5A and 5C). Adding blocking antibodies to MPCs cultured alone inhibited myotube formation, indicative of an autocrine activity (Figure 5E). These results demonstrate the direct involvement of APLN, OSM, and POSTN in

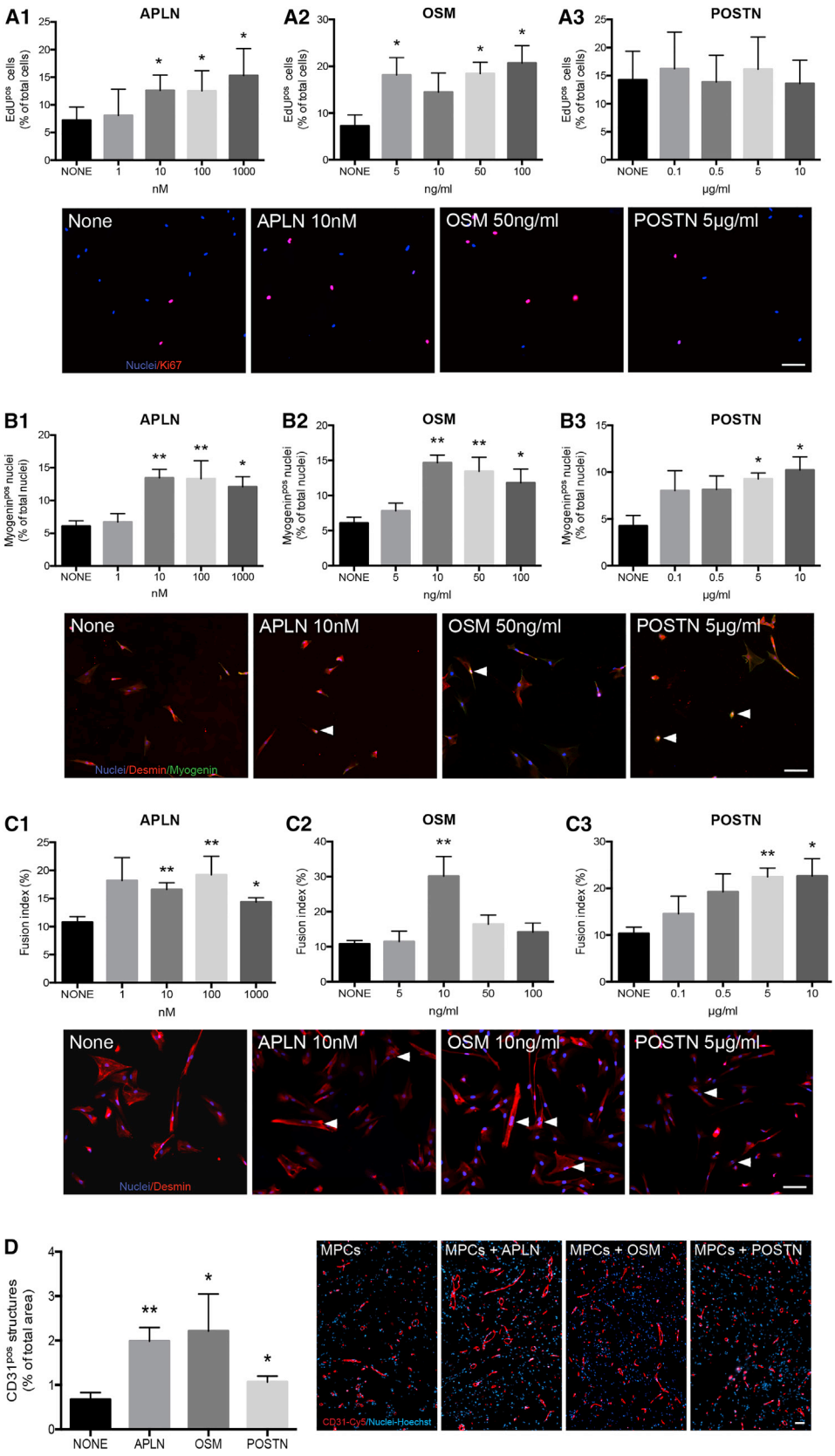

(legend on next page)

myogenesis/angiogenesis coupling, in addition to an autocrine effect occurring in MPCs.

Restorative Macrophages Stimulate Myogenesis/Angiogenesis Coupling

While the above molecular analysis was focused on ECs and SCs to demonstrate myogenesis/angiogenesis coupling, it is likely that other cell types may express a variety of molecules involved in this process. Macrophages and FAPs develop close interactions with MPCs (Joe et al., 2010; Saclier et al., 2013), and they are known to promote angiogenesis under some conditions (Hurley et al., 2010; Ochoa et al., 2007). RT-qPCR analysis on fluorescence-activated cell sorted populations in regenerating mouse muscle (Figure S4A) showed that *Apln* was mainly expressed by ECs (and to a lesser extent by SCs and FAPs), that *Osm* was mainly expressed by macrophages (and to a lesser extent by SCs), while *Postn* was mainly expressed by FAPs, although the four cell types did express the molecule at late stages of skeletal muscle regeneration (Figures S4B, and 6A–6C). Because FAPs have not been well characterized in human muscle and thus cannot be tested in *in vitro* models, the role of macrophages was investigated in the 3D assay. For this purpose, macrophages were seeded on top of the gel (Figure 6D), after having been activated by interleukin (IL)-4, to trigger alternative activation status, which is known to promote both myogenesis (Saclier et al., 2013) and angiogenesis (Jetten et al., 2014). Macrophages were also activated with IL-10/dexamethasone, which induces an anti-inflammatory status (Arnold et al., 2007; Saclier et al., 2013) closer to that of restorative macrophages in regenerating muscle (Varga et al., 2016). Figures 6E–6I shows that IL-4 and IL-10 anti-inflammatory macrophages stimulated the formation (+25% and +22%) of lumenized (+26% and +31%) capillaries by ECs and that of myotubes by MPCs (+49% and +29%). Blocking OSM blunted the stimulating effect of anti-inflammatory macrophages on capillary elongation (−13%) and severely inhibited their lumenization (−60%) (Figures 6E–6G) and the formation of myotubes (−68%) (Figures 6H and 6I), accounting for an inhibitory effect on macrophages and on ECs and MPCs as shown in Figure 5. These results indicate that anti-inflammatory macrophage-derived OSM regulates myogenesis/angiogenesis coupling.

Apelin, Oncostatin M, and Periostin Are Required for Myogenesis and Angiogenesis during Skeletal Muscle Regeneration

In vivo relevance of the role of APLN, OSM, or POSTN in myogenesis/angiogenesis coupling during skeletal muscle regeneration was evaluated in loss-of-function experiments. Because the molecules are secreted by several cell types, cell-specific KO models would not provide information. Therefore, experiments were performed using blocking antibodies or inhibitors injected intramuscularly at the time of the peak of expression of the molecules (Figure S3) (days 2–3 after cardiotoxin injury for APJ receptor antagonist [ML221] and anti-OSM antibodies and days 3–4 for anti-POSTN antibodies). Analysis at day 8 after injury included several criteria assessing the efficacy of myogenesis, as well as the capillarization of the myofibers assessing the efficacy of angiogenesis. Because APLN is considered to be the only ligand for APJ and APJ to be the only receptor for APLN, we considered that antagonizing APJ receptor mimics APLN blockade (Kang et al., 2013). APLN inhibition led to a decrease of the number of myogenin^{pos} cells (−28%, Figure 7A) as well as the number of nuclei/fiber (−20%, Figure 7B) and of embryonic myosin heavy chain (MyH3)^{pos}-regenerating myofibers (−31%, Figure 7C), indicative of reduced myogenic differentiation, fusion, and regeneration processes, respectively. As a result, the cross-sectional area (CSA) of the regenerating myofibers was smaller (−26%, Figure 7E). OSM inhibition induced a decrease in the number of both myogenin^{pos} cells (−31%, Figure 7A), nuclei/fibers (−13%, Figure 7B), MyH3^{pos} myofibers (−28%, Figure 7C), SCs (Pax7^{pos})/fiber (−25%, Figure 7D), and CSA of regenerating myofibers (−21%, Figure 7E). Similarly, inhibition of POSTN induced a decrease in all parameters (−60% of myogenin^{pos} cells [Figure 7A], −15% of the number of nuclei/fiber [Figure 7B], −27% of MyH3^{pos} myofibers [Figure 7C], −25% of SCs/fiber [Figures 7A and 7D], −14% of CSA [Figure 7E]). Finally, capillarization of the myofibers (i.e., the number of vessels/regenerating

Figure 4. APLN, OSM, and POSTN Gain-of-Function Experiments

(A–C) Human MPCs were treated with various concentrations of APLN (A1, B1, and C1), OSM (A2, B2, and C2), and POSTN (A3, B3, C3) (1–1,000 nM, 5–100 mg/mL, and 0.1–10 μg/mL, respectively). (A1–A3) MPC proliferation was evaluated using EdU labeling (red). (B1–B3) MPC differentiation was evaluated using labeling for desmin (red) and myogenin (green, arrowheads). (C1–C3) Fusion of differentiated myocytes was evaluated after immunolabeling for desmin (red). Arrowheads show myotubes.

(D) Matrigel plug assay was performed using MPCs with or without recombinant APLN (10 nM), OSM (50 ng/mL), or POSTN (5 μg/mL). Vessel structures were quantified after CD31 (red) labeling.

Blue, Hoechst. Mann-Whitney test was performed versus none: *$p < 0.05$; **$p < 0.01$. Results are means ± SEM of six and seven independent *in vitro* and *in vivo* experiments, respectively. Bars, 50 μm. See also Figures S1 and S2.

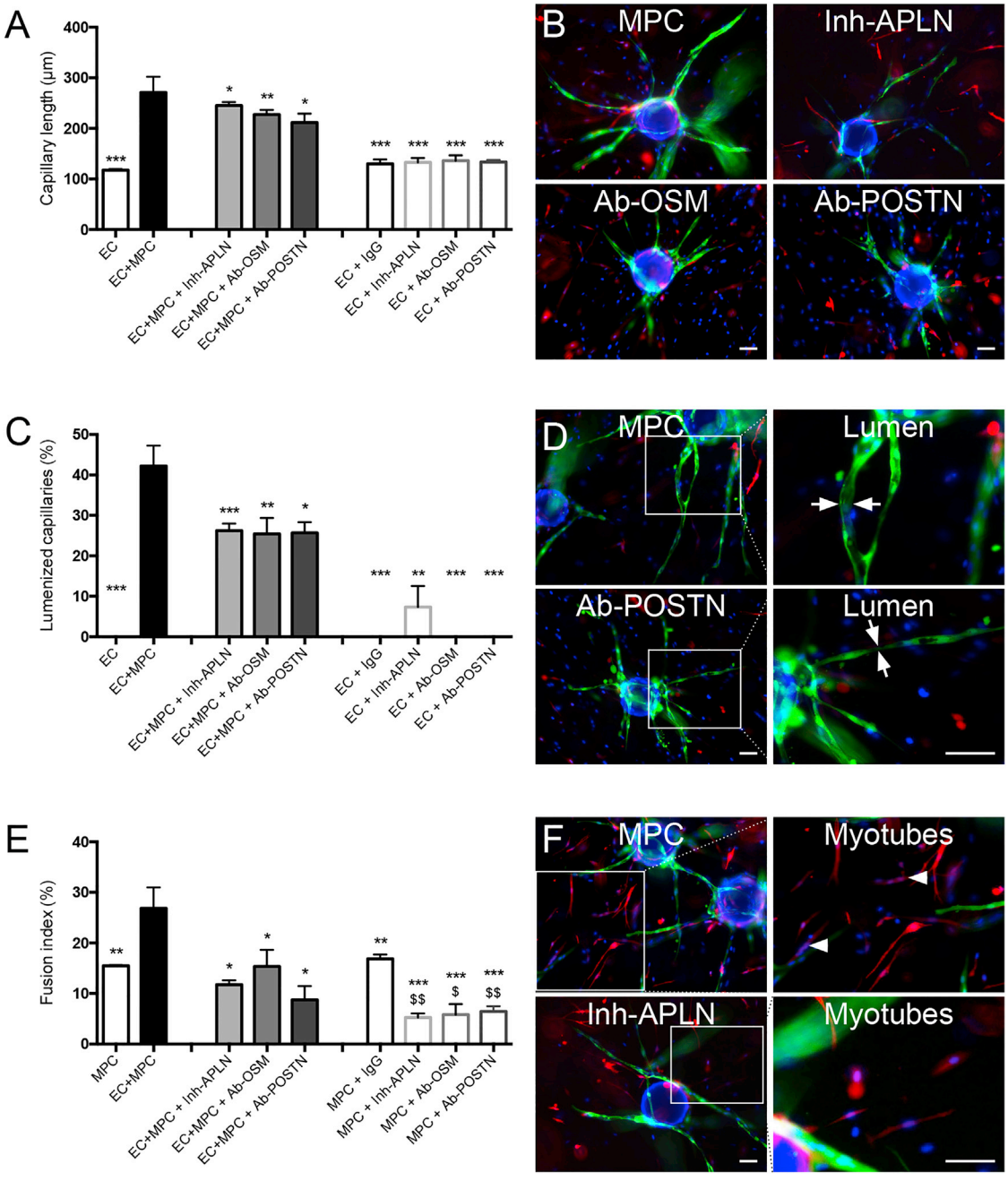

Figure 5. APLN, OSM, and POSTN Loss-of-Function Experiment on Myogenesis/Angiogenesis Coupling

The 3D assay used EC-GFP and RFP-MPCs that were embedded in the gel together or alone. In some experiments, IgGs, APLN receptor inhibitor ML221 (16 µM), anti-OSM, or anti-POSTN blocking antibodies (50 and 40 µg/mL) were added. Six days later, capillary length (A), lumenization (C), and myotube fusion (E) were evaluated. On the right, pictures present examples of capillary elongation (B), capillary lumenization (green, arrows) (D), and myotube formation (red, arrowheads) (F) in EC + MPC conditions with or without the inhibitors. Results are means ± SEM of at least three independent experiments. Mann-Whitney test was performed versus EC + MPC: *$p < 0.05$; **$p < 0.01$; ***$p < 0.001$; and versus MPC + IgG: $$p < 0.05$; $$$p < 0.01$. Bars, 100 µm. See also Figure S3.

myofiber) was decreased in all conditions (−22%, −23%, and −20% upon APLN, OSM, and POSTN inhibition, respectively) (Figure 7F). Collectively, these results show the requirement of the three secreted effectors in the control of the coupling of angiogenesis and myogenesis, which is required to achieve skeletal muscle regeneration.

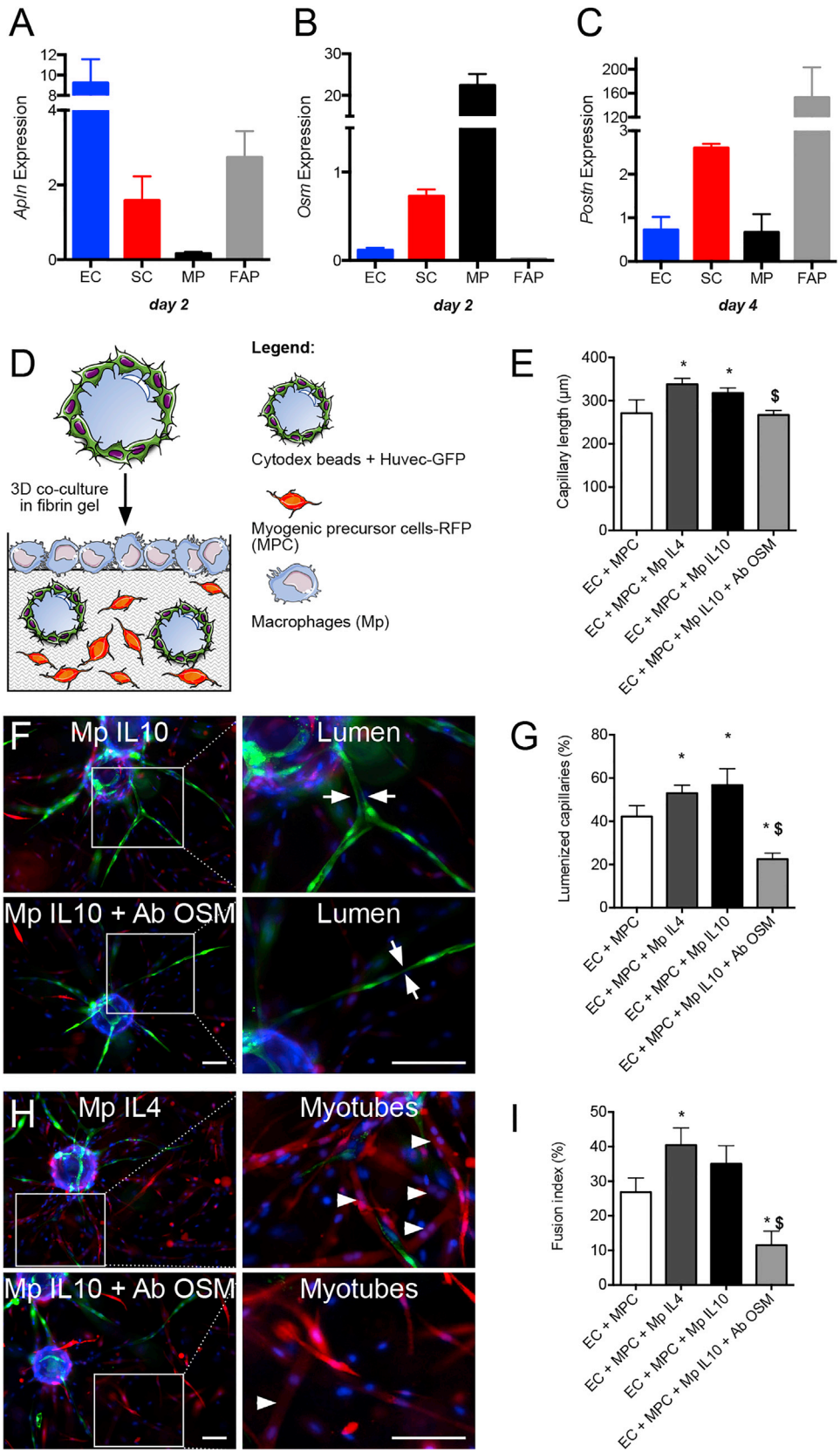

(legend on next page)

DISCUSSION

Our study demonstrates the functional interactions between ECs and MPCs underlying myogenesis/angiogenesis coupling during skeletal muscle regeneration. The two cell types reciprocally stimulated each other to promote angiogenesis and myogenesis *in vivo* and *in vitro*, showing that these two biological processes are coupled. Molecular profiling of ECs and SCs sorted from regenerating muscle allowed the identification of three effectors, APLN, OSM, and POSTN, that were shown to stimulate myogenesis/angiogenesis coupling and to be required for muscle regeneration. Furthermore, we described restorative macrophages as stimulators of myogenesis/angiogenesis coupling, notably through the secretion of OSM.

Previous studies identified bilateral relationships between MPCs and ECs (Christov et al., 2007; Rhoads et al., 2009). However, the present work identifies which steps of myogenesis are specifically controlled by ECs and dissects the pro-angiogenic properties of MPCs. Indeed, the 3D assay we used here encompasses the sequential steps of angiogenesis, recapitulating proliferation, sprouting, and lumen formation observed *in vivo*, which is not the case in the classic Matrigel *in vitro* assay (Nakatsu and Hughes, 2008). These results, coupled to the strong vessel formation in the *in vivo* Matrigel plug assay, definitively establish MPCs as pro-angiogenic cells. Notably, differentiated myocytes and myotubes strongly stimulated capillary morphogenesis. The analysis of cells cultured alone in the 3D model indicated that some weak autocrine activity drove the formation of short immature capillaries by ECS. MPCs alone formed myotubes but about 2-fold less efficiently than when ECs were present. This suggests that while an autocrine effect ensures basal myogenesis and angiogenesis, paracrine activities between ECs and MPCs strongly stimulate both processes, demonstrating the existence of a functional coupling of myogenesis with angiogenesis and explaining the previously observed concomitance of the two processes in regenerating muscle (Roberts and McGeachie, 1990).

Few studies investigated the molecular cross-talk between ECs and MPCs. EC-derived IGF-1, HGF, bFGF, PDGF-BB, and VEGF stimulate MPC growth *in vitro* (Christov et al., 2007; Rhoads et al., 2009) while Gli3, a Hedgehog (Hh) transcription factor, controls the cross-talk during ischemic muscle repair (Renault et al., 2013). Here, we restricted our transcriptomic analysis on effectors secreted by both ECs and SCs during skeletal muscle regeneration. Among the list (Table S1), several effectors were involved in the regulation of myogenesis or angiogenesis or in skeletal muscle regeneration, such as Osteopontin (Rowe et al., 2014), urokinase type plasminogen activator (Lluis et al., 2001), Galectin 1(Georgiadis et al., 2007), IL-6 (Serrano et al., 2008), and IGF-1 (Christov et al., 2007; Jetten et al., 2014). The screen identified three effectors, APLN, OSM, and POSTN, which were shown to stimulate myogenesis *in vitro* and angiogenesis *in vivo* in gain-of-function experiments. Moreover, blockade of these factors in the 3D coculture system strongly inhibited the formation of both myotubes and capillaries. Their blockade *in vivo* altered myogenesis and reduced angiogenesis in the regenerating muscle. The direct impact of APLN, OSM, and POSTN on both myogenesis and angiogenesis is thus necessary for driving efficient muscle regeneration.

The APLN/APJR axis is a known regulator of EC proliferation, sprouting, angiogenesis, vessel maturation, and size (Novakova et al., 2016). Our results identify a new function for APLN as a potent stimulator of myogenesis and confirmed its role in angiogenesis during tissue repair.

Matricellular POSTN expression is upregulated during myogenic differentiation *in vitro* (Ozdemir et al., 2014), in accordance with the expression profile we observed in SCs sorted from regenerating muscle. Consistently, POSTN stimulated the last steps of myogenesis, including differentiation and fusion. POSTN directly stimulated angiogenesis *in vivo*, in accordance with its positive effect on angiogenesis after limb ischemia (Kim et al., 2014). *In vivo*, POSTN was previously observed around newly forming myofibers, suggesting secretion by interstitial cells (Ozdemir et al., 2014). We showed that FAPs and SCs were the main providers of POSTN. Unfortunately, FAPs have not been characterized in normal human muscle yet so further *in vitro* investigations were not feasible.

The role of OSM in myogenesis has been documented in one report that indicates that OSM (ranging from 0.1 to 20 ng/mL) inhibits myogenesis of murine cells, through

Figure 6. Effect of Macrophages on Myogenesis/Angiogenesis Coupling

(A–C) Expression of *Apln* (A), *Osm* (B), and *Postn* (C) by ECs, SCs, macrophages (MP), and FAPs at day 2 and 4 of regeneration, as described in Figure S4.

(D, E, G, and I) 3D assay was performed with macrophages previously activated with interleukin (IL)-4 or IL-10/dexamethasone (DEX) layered on top of the gel (D). Six days later, capillary length (E), lumenization (G), and myotube formation (I) were quantified. In some experiments, anti-OSM blocking antibodies (50 μg/mL) were added.

(F and H) Representative pictures with capillary lumen formation (green, arrows) and myotube formation (red, arrowheads).

Results are means ± SEM of four to six independent experiments. Mann-Whitney test was performed versus none: *$p < 0.05$; and versus Mp + IL10: \$$p < 0.05$. Bars, 100 μm.

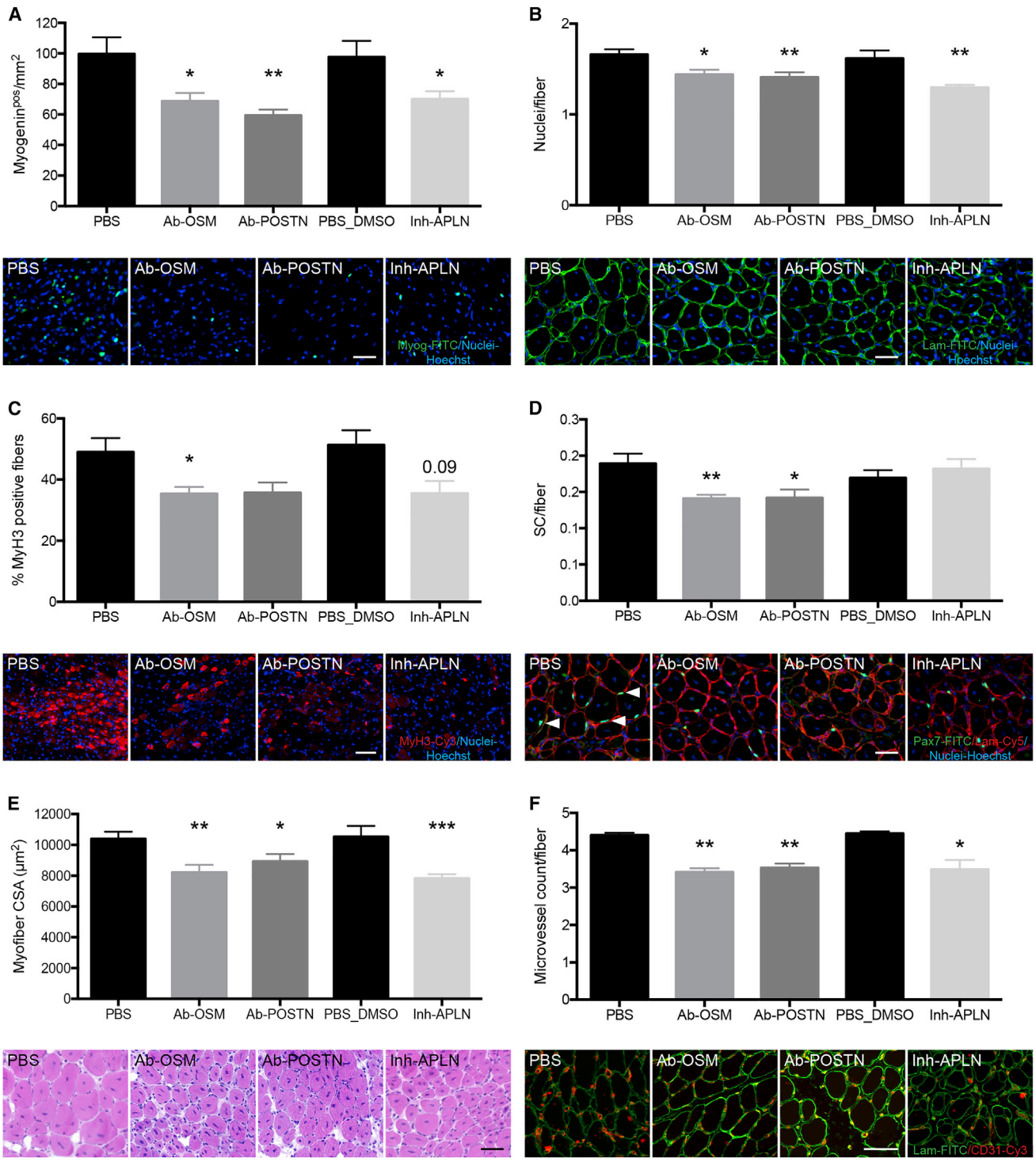

Figure 7. *In Vivo* APLN, OSM, and POSTN Loss-of-Function Experiments during Skeletal Muscle Regeneration

Tibialis anterior muscles were injected with cardiotoxin. APLN receptor inhibitor (16 μM) and anti-OSM blocking antibodies (5 μg) were injected intramuscularly at days 2 and 3 post injury, while anti-POSTN blocking antibodies (5 μg) were injected intramuscularly at days 3 and 4 post injury. Muscles were recovered at day 8. The following criteria were evaluated: (A) number of myogenin^{pos} cells/mm^2 (in pictures myogenin is green); (B) number of nuclei/fiber (in pictures laminin is green); (C) number of embryonic myosin heavy chain (MyH3)^{pos}

(legend continued on next page)

gp130/OSMR and the JAK1/STAT1/STAT3 pathway (Xiao et al., 2011). The present study utilized higher doses of OSM (from 5 to 200 ng/mL) and human MPCs, which respond to OSM through both gp130/LIFR and gp130/OSMR receptors (Thoma et al., 1994). In this context, OSM stimulated all steps of myogenesis *in vitro*. Although dissecting the effects of OSM on each step of myogenesis would require a study in itself, we may assume that different OSM concentrations have, in combination with the FBS compounds present in the culture, various effects on MPCs. Some molecules were previously reported to oppositely stimulate MPC proliferation depending on their concentration (e.g., tumor necrosis factor alpha [TNF-α]; Li, 2003), and some molecules trigger opposite effects on different cell populations within the MPC culture (e.g., Angiopoetin-1 induces both self-renewal and differentiation; Abou-Khalil et al., 2009). Similar contrasting results have been reported for the effects of OSM on angiogenesis, reporting inhibitory (Takashima and Klagsbrun, 1996) and stimulating effects (Vasse et al., 1999; Wijelath et al., 1997). OSM effects certainly depend on its local concentration in the close environment, which may explain the discrepancy between these studies. However, our *in vitro* and *in vivo* loss-of-function studies clearly showed inhibition of both myogenesis and angiogenesis.

Macrophages were the main producers of OSM during skeletal muscle regeneration, as shown in other repairing tissues (Ganesh et al., 2012; Guihard et al., 2015). *Osm* expression is higher in recovery than in inflammatory macrophages (gene expression analysis in Varga et al., 2016). Accordingly, blocking OSM inhibited the myogenesis/angiogenesis coupling induced by restorative macrophages in the 3D *in vitro* assay. Our previous work identified anti-inflammatory/restorative macrophages as supportive cells for MPC differentiation and fusion and as required for efficient muscle regeneration (Arnold et al., 2007; Mounier et al., 2013; Saclier et al., 2013). Macrophage angiogenic properties are less well documented in tissue repair, since they may secrete both pro-angiogenic or angiostatic factors (Rahat et al., 2014). Anti-inflammatory macrophages were shown to be more angiogenic than their pro-inflammatory counterparts (Jetten et al., 2014) but other studies reported an anti-angiogenic role of IL-4-activated macrophages (Wu et al., 2015) and pro-angiogenic activity of pro-inflammatory macrophages (Tattersall et al., 2016). Physical interactions between macrophages and ECs seem important in the branching during angiogenesis sprouting (Tattersall et al., 2016) or "bridging sprouts" (Corliss et al., 2016). *In vivo,* animals deficient in 5′-AMP-activated protein kinase (AMPK) α1 in macrophages exhibit reduced remodeling of collateral arterioles after femoral artery ligation (Zhu et al., 2016), which may be explained by the defect in the acquisition of the restorative phenotype we previously reported (Mounier et al., 2013). Still *in vivo*, reduced macrophage infiltration in the injured muscle is associated with reduced angiogenesis (Ochoa et al., 2007; Zordan et al., 2014).

These results highlight the complexity of the cellular interactions that occur during tissue repair and reveal restorative macrophages as playing key roles in orchestrating concomitant parenchyma recovery (myogenesis and myofiber fusion) (Saclier et al., 2013), vascular bed recovery (angiogenesis), as well as matrix remodeling (through their action on FAPs; Lemos et al., 2015), to promote efficient skeletal muscle regeneration.

EXPERIMENTAL PROCEDURES

Human MPC Culture

Human MPCs were isolated from normal adult skeletal muscle samples according to French legislation (protocol registered at the Agence de la Biomedecine #DC-2009-944) as previously described (Saclier et al., 2013). Conditioned medium was recovered after 24 hr in advanced RPMI 1640 medium (Gibco) containing 0.5% FBS. Differentiated myocytes were obtained after 72 hr of culture in HAMF12 medium containing 5% FBS. Myotubes were obtained from 72 hr cultures of myocytes. In some experiments, MPCs were transduced with RFP lentivirus.

Human Umbilical Vein Endothelial Cell Culture

Human umbilical vein endothelial cells (HUVECs) were obtained from Promocell and cultured in ECGM-2 complete medium (Promocell). They were transduced with GFP lentivirus. Conditioned medium was recovered after 24 hr culture in advanced RPMI 1640 medium containing 0.5% FBS.

Migration Assay

Migration was performed using two-chamber Ibidi inserts (Ibidi GmbH). Each chamber was filled with MPCs or for 8–12 hr. Silicone walls were removed, and the gap between the two cell types was imaged at 0 and 24 hr.

Proliferation Assay

Cells were seeded in multi-well plates and conditioned medium of the other cell type was added for 24 hr in the absence or presence of

fibers (in pictures MyH3 is red); (D) number of $Pax7^{pos}$ (SCs)/fiber (in pictures Pax7 is green [arrowheads] and laminin is red); (E) cross-sectional area (CSA) of the regenerating myofibers (H&E staining); (F) number of vessels/myofiber (in pictures CD31 is red and laminin is green). Blue, Hoechst. Bars, 50 μm. Mann-Whitney test was performed versus PBS for Ab-OSM and Ab-POSTN and versus PBS-DMSO for Inh-APLN: *$p < 0.05$; **$p < 0.01$; ***$p < 0.001$. Results are means ± SEM of six independent experiments.

recombinant proteins. Ki67 immunolabeling or ethinyl deoxyuridine (EdU) staining was then performed.

Myogenic Differentiation

HUVEC-conditioned medium was added to MPCs in the presence or the absence of recombinant proteins for 72 hr. Myogenin immunolabeling was performed.

Myogenic Fusion

HUVEC-conditioned medium was added for 72 hr on myocytes in the presence or absence of recombinant proteins. Desmin immunolabeling was performed.

3D *In Vitro* Angiogenesis Assay

HUVEC-GFPs were combined with the cytodex beads and combined in the pre-gel solution as described previously (Ferratge et al., 2017). MPCs, myocytes, or myotubes were added to the pre-gel. In some experiments, ECs or MPCs were seeded alone, and IgG, blocking antibodies, or inhibitors were added to the pre-gel. Human dermal fibroblasts (NHDF, Promocell) or MPCs or macrophages were seeded on top of the gel. The cells were cultured in EndoGro medium for up to 6 days.

In Vivo Muscle Regeneration

Tibialis anterior muscle was injected with cardiotoxin and recovered for histological analysis at day 8 as described previously (Mounier et al., 2013). In some experiments, blocking antibodies or inhibitors were injected intramuscularly. Muscle cryosections were immunolabeled using anti-laminin, CD31, Ki67, Pax7, Myogenin, and MyH3 antibodies.

In Vivo Angiogenesis Assay

Adult male C57BL/6 mice were bred and used in compliance with French and European regulations. The principal investigators are licensed for these experiments, and the protocols were approved by local Animal Care and Use Committee and the French Ministery of Agriculture. Murine MPCs were cultured as described previously (Mounier et al., 2013). NIH3T3cells were cultured in DMEM containing 15% FBS. Cells were embedded in cold Matrigel and 500 μL of the mix was injected subcutaneously in 4- to 6-week-old male C57BL/6 mice. In some experiments, recombinant proteins were added. After 21 days, mice were euthanized, and plugs were recovered and fixed. Sections were treated with anti-CD31, desmin, and α-SMA antibodies. Functional angiogenesis inside the plug was evaluated as the amount of hemoglobin using Drabkin's reagent.

Cell Sorting from Regenerating Muscle

Single-cell suspensions were obtained from muscles by enzymatic digestion. ECs, SCs, macrophages, and FAPs were isolated using anti-CD45 PE, F4-80 APC-Cy7, CD34-FITC, Sca1-eFluor 605 or PerCP-Cy5.5, α7-integrin-APC, CD31-eFluor 450, and PDGFRα (CD140a) PE-Cy7 antibodies.

Transcriptomic Analysis

Total RNAs were extracted from sorted ECs or MPCs using an RNeasy Mini Kit (QIAGEN). RNA integrity was checked on an Agilent Bioanalyzer 2100. Global expression data were obtained using Affymetrix GeneChip Mouse Gene 2.0 ST arrays. The microarray data are publicly available (GEO: GSE103684). Data were robust multichip average normalized and were first controlled and analyzed in an unsupervised way by principal component analysis, and a one-way ANOVA was applied to extract DEGs using PartekGS software. Cluster analysis and enrichment were made using DAVID and Pathway Studio software (the strategy is presented in Figure S1J). A list of genes expressed by both ECs and MPCs was finalized (Table S1).

Statistics

All experiments were performed in at least three independent experiments, i.e., different primary cultures or different animals. The exact number of experiments and statistical significance are given in the figure legends. Results are expressed as means ± SEM. Means were compared using Mann-Whitney or two-way ANOVA and Sidak post tests.

ACCESSION NUMBERS

The microarray data are publicly available (GEO: GSE103684).

SUPPLEMENTAL INFORMATION

Supplemental Information includes Supplemental Experimental Procedures, four figures, and two tables and can be found with this article online at https://doi.org/10.1016/j.stemcr.2017.10.027.

AUTHOR CONTRIBUTIONS

Conceptualization, B.C. and S.G.; Methodology, B.C., C.L., L.M., R.M., and S.G.; Validation, B.C. and C.L.; Formal Analysis, B.C. and C.L.; Investigation, C.G., C.L., M.M., M.W.-G., N.V., P.B., P.L., R.A.-K., R.M., S.B.-L., and S.L.; Resources, B.C., F.C., L.M., R.M., and S.G.; Data Curation, B.C. and C.L.; Writing – Original Draft, B.C. and C.L.; Writing – Review & Editing, B.C., C.G., C.L., M.W.-G., N.V., P.B., P.L., R.A.-K., R.M., S.G., and S.L.; Visualization, B.C. and C.L.; Supervision, B.C. and R.M.; Project Administration, B.C.; Funding Acquisition, B.C. and F.C.

ACKNOWLEDGMENTS

This work was funded by INSERM, CNRS, Université Paris Descartes, and Université Claude Bernard Lyon 1, by EU FP7 Endostem (no. 241440), and by Association Française contre les Myopathies (grant no. 18003). C.L. was supported by Dim Stem Pole from Région Ile-de-France and Association Française contre les Myopathies. R.A.-K. was supported by Association Française contre les Myopathies. C.G. was supported by a Poste d'Accueil APHP/CNRS. We thank AniRA-Cytometry facility from SFR Biosciences, Université Claude Bernard Lyon 1, and Genom'ic facility from Institut Cochin.

Received: May 24, 2017
Revised: October 27, 2017
Accepted: October 30, 2017
Published: November 30, 2017

REFERENCES

Abou-Khalil, R., Le Grand, F., Pallafacchina, G., Valable, S., Authier, F.J., Rudnicki, M.A., Gherardi, R.K., Germain, S., Chretien, F., Sotiropoulos, A., et al. (2009). Autocrine and paracrine Angiopoietin 1/Tie-2 signalling promotes muscle satellite cell self-renewal. Cell Stem Cell *5*, 298–309.

Arnold, L., Henry, A., Poron, F., Baba-Amer, Y., van Rooijen, N., Plonquet, A., Gherardi, R.K., and Chazaud, B. (2007). Inflammatory monocytes recruited after skeletal muscle injury switch into antiinflammatory macrophages to support myogenesis. J. Exp. Med. *204*, 1071–1081.

Arsic, N., Zacchigna, S., Zentilin, L., Ramirez-Correa, G., Pattarini, L., Salvi, A., Sinagra, G., and Giacca, M. (2004). Vascular endothelial growth factor stimulates skeletal muscle regeneration in vivo. Mol. Ther. *10*, 844–854.

Borselli, C., Storrie, H., Benesch-Lee, F., Shvartsman, D., Cezar, C., Lichtman, J.W., Vandenburgh, H.H., and Mooney, D.J. (2010). Functional muscle regeneration with combined delivery of angiogenesis and myogenesis factors. Proc. Natl. Acad. Sci. USA *107*, 3287–3292.

Bryan, B.A., Walshe, T.E., Mitchell, D.C., Havumaki, J.S., Saint-Geniez, M., Maharaj, A.S., Maldonado, A.E., and D'Amore, P.A. (2008). Coordinated vascular endothelial growth factor expression and signaling during skeletal myogenic differentiation. Mol. Biol. Cell *19*, 994–1006.

Butcher, J.T., Norris, R.A., Hoffman, S., Mjaatvedt, C.H., and Markwald, R.R. (2007). Periostin promotes atrioventricular mesenchyme matrix invasion and remodeling mediated by integrin signaling through Rho/PI 3-kinase. Dev. Biol. *302*, 256–266.

Christov, C., Chretien, F., Abou-Khalil, R., Bassez, G., Vallet, G., Authier, F.J., Bassaglia, Y., Shinin, V., Tajbakhsh, S., Chazaud, B., et al. (2007). Muscle satellite cells and endothelial cells: close neighbors and privileged partners. Mol. Biol. Cell *18*, 1397–1409.

Corliss, B.A., Azimi, M.S., Munson, J.M., Peirce, S.M., and Murfee, W.L. (2016). Macrophages: an inflammatory link between angiogenesis and lymphangiogenesis. Microcirculation *23*, 95–121.

Ferratge, S., Ha, G., Carpentier, G., Arouche, N., Bascetin, R., Muller, L., Germain, S., and Uzan, G. (2017). Initial clonogenic potential of human endothelial progenitor cells is predictive of their further properties and establishes a functional hierarchy related to immaturity. Stem Cell Res. *21*, 148–159.

Ganesh, K., Das, A., Dickerson, R., Khanna, S., Parinandi, N.L., Gordillo, G.M., Sen, C.K., and Roy, S. (2012). Prostaglandin E(2) induces oncostatin M expression in human chronic wound macrophages through Axl receptor tyrosine kinase pathway. J. Immunol. *189*, 2563–2573.

Georgiadis, V., Stewart, H.J., Pollard, H.J., Tavsanoglu, Y., Prasad, R., Horwood, J., Deltour, L., Goldring, K., Poirier, F., and Lawrence-Watt, D.J. (2007). Lack of galectin-1 results in defects in myoblast fusion and muscle regeneration. Dev. Dyn. *236*, 1014–1024.

Germani, A., Di Carlo, A., Mangoni, A., Straino, S., Giacinti, C., Turrini, P., Biglioli, P., and Capogrossi, M.C. (2003). Vascular endothelial growth factor modulates skeletal myoblast function. Am. J. Pathol. *163*, 1417–1428.

Gitiaux, C., Kostallari, E., Lafuste, P., Authier, F.J., Christov, C., and Gherardi, R.K. (2013). Whole microvascular unit deletions in dermatomyositis. Ann. Rheum. Dis. *72*, 445–452.

Gitiaux, C., De Antonio, M., Aouizerate, J., Gherardi, R.K., Guilbert, T., Barnerias, C., Bodemer, C., Brochard-Payet, K., Quartier, P., Musset, L., et al. (2016). Vasculopathy-related clinical and pathological features are associated with severe juvenile dermatomyositis. Rheumatology (Oxford) *55*, 470–479.

Guihard, P., Boutet, M.A., Brounais-Le Royer, B., Gamblin, A.L., Amiaud, J., Renaud, A., Berreur, M., Redini, F., Heymann, D., Layrolle, P., et al. (2015). Oncostatin m, an inflammatory cytokine produced by macrophages, supports intramembranous bone healing in a mouse model of tibia injury. Am. J. Pathol. *185*, 765–775.

Hansen-Smith, F.M., Hudlicka, O., and Egginton, S. (1996). In vivo angiogenesis in adult rat skeletal muscle: early changes in capillary network architecture and ultrastructure. Cell Tissue Res. *286*, 123–136.

Hardy, D., Besnard, A., Latil, M., Jouvion, G., Briand, D., Thepenier, C., Pascal, Q., Guguin, A., Gayraud-Morel, B., Cavaillon, J.M., et al. (2016). Comparative study of injury models for studying muscle regeneration in mice. PLoS One *11*, e0147198.

Hurley, J.R., Balaji, S., and Narmoneva, D.A. (2010). Complex temporal regulation of capillary morphogenesis by fibroblasts. Am. J. Physiol. Cell Physiol. *299*, C444–C453.

Ito, Y., Iwamoto, Y., Tanaka, K., Okuyama, K., and Sugioka, Y. (1996). A quantitative assay using basement membrane extracts to study tumor angiogenesis in vivo. Int. J. Cancer *67*, 148–152.

Jetten, N., Verbruggen, S., Gijbels, M.J., Post, M.J., De Winther, M.P., and Donners, M.M. (2014). Anti-inflammatory M2, but not pro-inflammatory M1 macrophages promote angiogenesis in vivo. Angiogenesis *17*, 109–118.

Joe, A.W., Yi, L., Natarajan, A., Le Grand, F., So, L., Wang, J., Rudnicki, M.A., and Rossi, F.M. (2010). Muscle injury activates resident fibro/adipogenic progenitors that facilitate myogenesis. Nat. Cell Biol. *12*, 153–163.

Kang, Y., Kim, J., Anderson, J.P., Wu, J., Gleim, S.R., Kundu, R.K., McLean, D.L., Kim, J.D., Park, H., Jin, S.W., et al. (2013). Apelin-APJ signaling is a critical regulator of endothelial MEF2 activation in cardiovascular development. Circ. Res. *113*, 22–31.

Kim, B.R., Jang, I.H., Shin, S.H., Kwon, Y.W., Heo, S.C., Choi, E.J., Lee, J.S., and Kim, J.H. (2014). Therapeutic angiogenesis in a murine model of limb ischemia by recombinant periostin and its fasciclin I domain. Biochim. Biophys. Acta *1842*, 1324–1332.

Latroche, C., Gitiaux, C., Chretien, F., Desguerre, I., Mounier, R., and Chazaud, B. (2015a). Skeletal muscle microvasculature: a highly dynamic lifeline. Physiology *30*, 417–427.

Latroche, C., Matot, B., Martins-Bach, A., Briand, D., Chazaud, B., Wary, C., Carlier, P.G., Chretien, F., and Jouvion, G. (2015b). Structural and functional alterations of skeletal muscle microvasculature in dystrophin-deficient mdx mice. Am. J. Pathol. *185*, 2482–2494.

Lemos, D.R., Babaeijandaghi, F., Low, M., Chang, C.K., Lee, S.T., Fiore, D., Zhang, R.H., Natarajan, A., Nedospasov, S.A., and Rossi, F.M. (2015). Nilotinib reduces muscle fibrosis in chronic muscle injury by promoting TNF-mediated apoptosis of fibro/adipogenic progenitors. Nat. Med. *21*, 786–794.

Li, Y.P. (2003). TNF-{alpha} is a mitogen in skeletal muscle. Am. J. Physiol. Cell Physiol. *285*, C370–C376.

Lluis, F., Roma, J., Suelves, M., Parra, M., Aniorte, G., Gallardo, E., Illa, I., Rodriguez, L., Hughes, S.M., Carmeliet, P., et al. (2001). Urokinase-dependent plasminogen activation is required for efficient skeletal muscle regeneration in vivo. Blood *97*, 1703–1711.

Mounier, R., Theret, M., Arnold, L., Cuvellier, S., Bultot, L., Goransson, O., Sanz, N., Ferry, A., Sakamoto, K., Foretz, M., et al. (2013). AMPKalpha1 regulates macrophage skewing at the time of resolution of inflammation during skeletal muscle regeneration. Cell Metab. *18*, 251–264.

Nakatsu, M.N., and Hughes, C.C. (2008). An optimized three-dimensional in vitro model for the analysis of angiogenesis. Methods Enzymol. *443*, 65–82.

Novakova, V., Sandhu, G.S., Dragomir-Daescu, D., and Klabusay, M. (2016). Apelinergic system in endothelial cells and its role in angiogenesis in myocardial ischemia. Vascul. Pharmacol. *76*, 1–10.

Ochoa, O., Sun, D., Reyes-Reyna, S.M., Waite, L.L., Michalek, J.E., McManus, L.M., and Shireman, P.K. (2007). Delayed angiogenesis and VEGF production in CCR2-/- mice during impaired skeletal muscle regeneration. Am. J. Physiol. Reg. Int. Comp. Physiol. *293*, R651–R661.

Ozdemir, C., Akpulat, U., Sharafi, P., Yildiz, Y., Onbasilar, I., and Kocaefe, C. (2014). Periostin is temporally expressed as an extracellular matrix component in skeletal muscle regeneration and differentiation. Gene *553*, 130–139.

Pannerec, A., Marazzi, G., and Sassoon, D. (2012). Stem cells in the hood: the skeletal muscle niche. Trends Mol. Med. *18*, 599–606.

Rahat, M.A., Hemmerlein, B., and Iragavarapu-Charyulu, V. (2014). The regulation of angiogenesis by tissue cell-macrophage interactions. Front. Physiol. *5*, 262.

Ralston, E., Lu, Z., Biscocho, N., Soumaka, E., Mavroidis, M., Prats, C., Lomo, T., Capetanaki, Y., and Ploug, T. (2006). Blood vessels and desmin control the positioning of nuclei in skeletal muscle fibers. J. Cell Physiol. *209*, 874–882.

Renault, M.A., Vandierdonck, S., Chapouly, C., Yu, Y., Qin, G., Metras, A., Couffinhal, T., Losordo, D.W., Yao, Q., Reynaud, A., et al. (2013). Gli3 regulation of myogenesis is necessary for ischemia-induced angiogenesis. Circ. Res. *113*, 1148–1158.

Rhoads, R.P., Johnson, R.M., Rathbone, C.R., Liu, X., Temm-Grove, C.J., Sheehan, S.M., Hoying, J.B., and Allen, R.E. (2009). Satellite cell-mediated angiogenesis coincides with a functional hypoxia-inducible factor (HIF) pathway. Am. J. Physiol. Cell Physiol. *296*, C1321–C1328.

Roberts, P., and McGeachie, J.K. (1990). Endothelial cell activation during angiogenesis in freely transplanted skeletal muscles in mice and its relationship to the onset of myogenesis. J. Anat. *169*, 197–207.

Rowe, G.C., Raghuram, S., Jang, C., Nagy, J.A., Patten, I.S., Goyal, A., Chan, M.C., Liu, L.X., Jiang, A., Spokes, K.C., et al. (2014). PGC-1alpha induces SPP1 to activate macrophages and orchestrate functional angiogenesis in skeletal muscle. Circ. Res. *115*, 504–517.

Saclier, M., Yacoub-Youssef, H., Mackey, A.L., Arnold, L., Ardjoune, H., Magnan, M., Sailhan, F., Chelly, J., Pavlath, G.K., Mounier, R., et al. (2013). Differentially activated macrophages orchestrate myogenic precursor cell fate during human skeletal muscle regeneration. Stem Cells *31*, 384–396.

Serrano, A.L., Baeza-Raja, B., Perdiguero, E., Jardi, M., and Munoz-Canoves, P. (2008). Interleukin-6 is an essential regulator of satellite cell-mediated skeletal muscle hypertrophy. Cell Metab. *7*, 33–44.

Takashima, S., and Klagsbrun, M. (1996). Inhibition of endothelial cell growth by macrophage-like U-937 cell-derived oncostatin M, leukemia inhibitory factor, and transforming growth factor beta1. J. Biol. Chem. *271*, 24901–24906.

Tattersall, I.W., Du, J., Cong, Z., Cho, B.S., Klein, A.M., Dieck, C.L., Chaudhri, R.A., Cuervo, H., Herts, J.H., and Kitajewski, J. (2016). In vitro modeling of endothelial interaction with macrophages and pericytes demonstrates Notch signaling function in the vascular microenvironment. Angiogenesis *19*, 201–215.

Thoma, B., Bird, T.A., Friend, D.J., Gearing, D.P., and Dower, S.K. (1994). Oncostatin M and leukemia inhibitory factor trigger overlapping and different signals through partially shared receptor complexes. J. Biol. Chem. *269*, 6215–6222.

Uezumi, A., Fukada, S., Yamamoto, N., Takeda, S., and Tsuchida, K. (2010). Mesenchymal progenitors distinct from satellite cells contribute to ectopic fat cell formation in skeletal muscle. Nat. Cell Biol. *12*, 143–152.

Varga, T., Mounier, R., Horvath, A., Cuvellier, S., Dumont, F., Poliska, S., Ardjoune, H., Juban, G., Nagy, L., and Chazaud, B. (2016). Highly dynamic transcriptional signature of distinct macrophage subsets during sterile inflammation, resolution, and tissue repair. J. Immunol. *196*, 4771–4782.

Vasse, M., Pourtau, J., Trochon, V., Muraine, M., Vannier, J.P., Lu, H., Soria, J., and Soria, C. (1999). Oncostatin M induces angiogenesis in vitro and in vivo. Arterioscler. Thromb. Vasc. Biol. *19*, 1835–1842.

Wijelath, E.S., Carlsen, B., Cole, T., Chen, J., Kothari, S., and Hammond, W.P. (1997). Oncostatin M induces basic fibroblast growth factor expression in endothelial cells and promotes endothelial cell proliferation, migration and spindle morphology. J. Cell Sci. *110*, 871–879.

Wu, W.K., Georgiadis, A., Copland, D.A., Liyanage, S., Luhmann, U.F., Robbie, S.J., Liu, J., Wu, J., Bainbridge, J.W., Bates, D.O., et al. (2015). IL-4 regulates specific Arg-1(+) macrophage sFlt-1-mediated inhibition of angiogenesis. Am. J. Pathol. *185*, 2324–2335.

Xiao, F., Wang, H., Fu, X., Li, Y., Ma, K., Sun, L., Gao, X., and Wu, Z. (2011). Oncostatin M inhibits myoblast differentiation and regulates muscle regeneration. Cell Res. *21*, 350–364.

Yin, H., Price, F., and Rudnicki, M.A. (2013). Satellite cells and the muscle stem cell niche. Physiol. Rev. *93*, 23–67.

Zhu, H., Zhang, M., Liu, Z., Xing, J., Moriasi, C., Dai, X., and Zou, M.H. (2016). AMP-activated protein kinase alpha1 in macrophages promotes collateral remodeling and arteriogenesis in mice in vivo. Arterioscler. Thromb. Vasc. Biol. *36*, 1868–1878.

Zordan, P., Rigamonti, E., Freudenberg, K., Conti, V., Azzoni, E., Rovere-Querini, P., and Brunelli, S. (2014). Macrophages commit postnatal endothelium-derived progenitors to angiogenesis and restrict endothelial to mesenchymal transition during muscle regeneration. Cell Death Dis. *5*, e1031.

Stem Cell Reports, Volume *9*

Supplemental Information

Coupling between Myogenesis and Angiogenesis during Skeletal Muscle Regeneration Is Stimulated by Restorative Macrophages

Claire Latroche, Michèle Weiss-Gayet, Laurent Muller, Cyril Gitiaux, Pascal Leblanc, Sophie Liot, Sabrina Ben-Larbi, Rana Abou-Khalil, Nicolas Verger, Paul Bardot, Mélanie Magnan, Fabrice Chrétien, Rémi Mounier, Stéphane Germain, and Bénédicte Chazaud

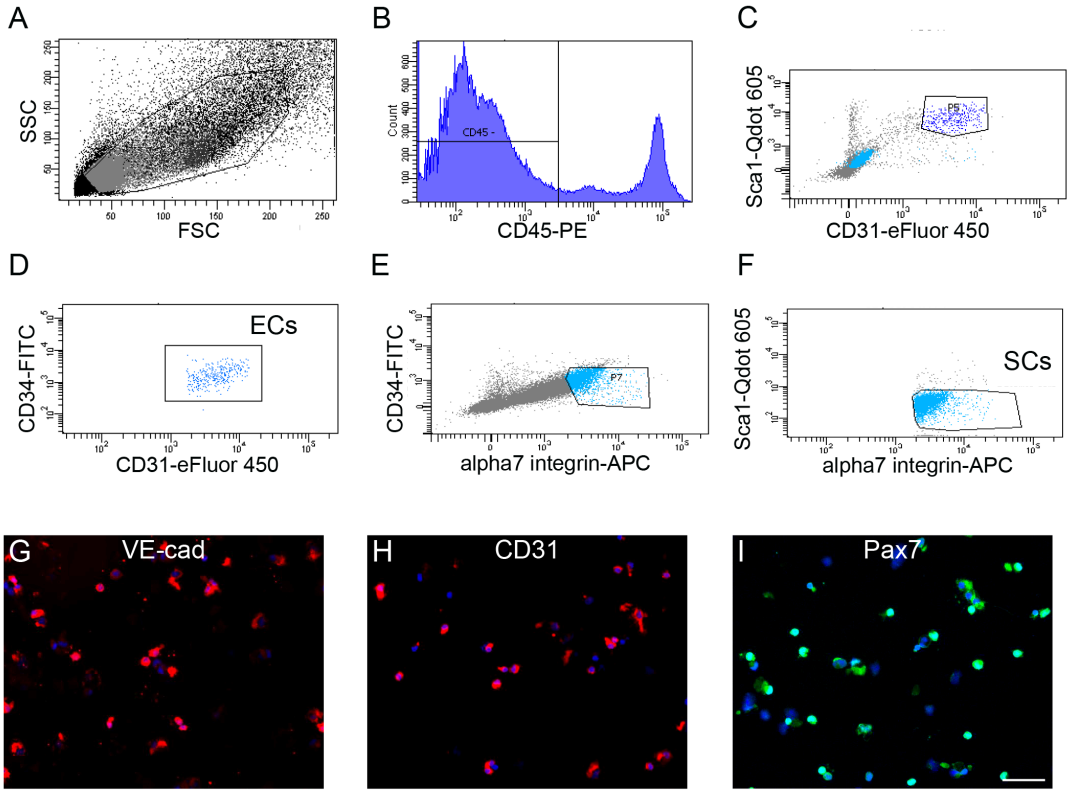

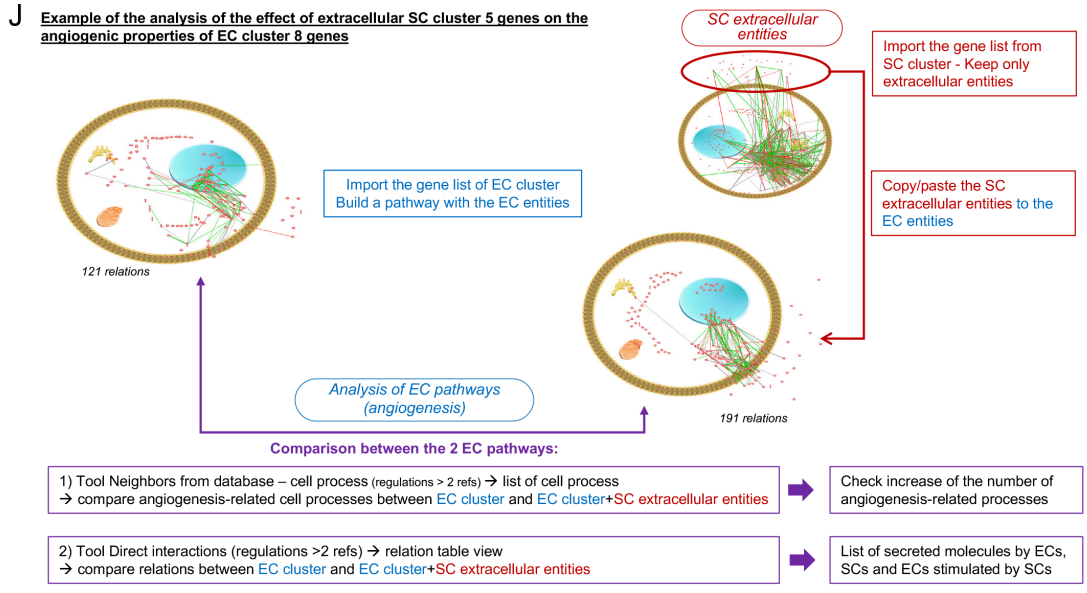

List of analyses that were performed:

Extracellular entities of:	*SC clusters 1, 5 (enriched in GO angiogenesis)*	*EC clusters 2, 4, 5, 7 (enriched in GO myogenesis)*
were tested on:	*EC clusters 2, 4, 5, 6, 7, 8 (enriched in GO angiogenesis)*	*SC clusters 3, 4, 5 (enriched in GO myogenesis)*
For properties on:	*angiogenesis*	*myogenesis*

Figure S1, related to Fig.4. Analysis of genes expressed by ECs and SCs during muscle regeneration. (A-F) Gating strategy for the FACS-sorting of ECs and SCs from regenerating *Tibialis Anterior* mouse muscle. (A) Total cell SSC/FSC representation. (B) Hematopoietic cells ($CD45^{pos}$) were excluded. (C) ECs were gated as Sca1+ CD34+ CD31+, (D) plot shows the purity of the sorted EC population. (E) SCs were isolated as CD45- CD34+ Sca1- α7-integrin+, (F) plot shows the purity of the sorted SC population. (G-I) Sorted cells were cytospined and immunostained with VE-cad (G) or CD31 (H) antibodies for ECs and Pax7 (I) antibodies for SCs (Blue=Hoechst). Bar = 50 µm. (J) Flow chart strategy for the analysis of genes expressed by ECs and SCs in regenerating muscle using Pathway Studio software. See also Figures 4, 5, 7 for the functional analysis.

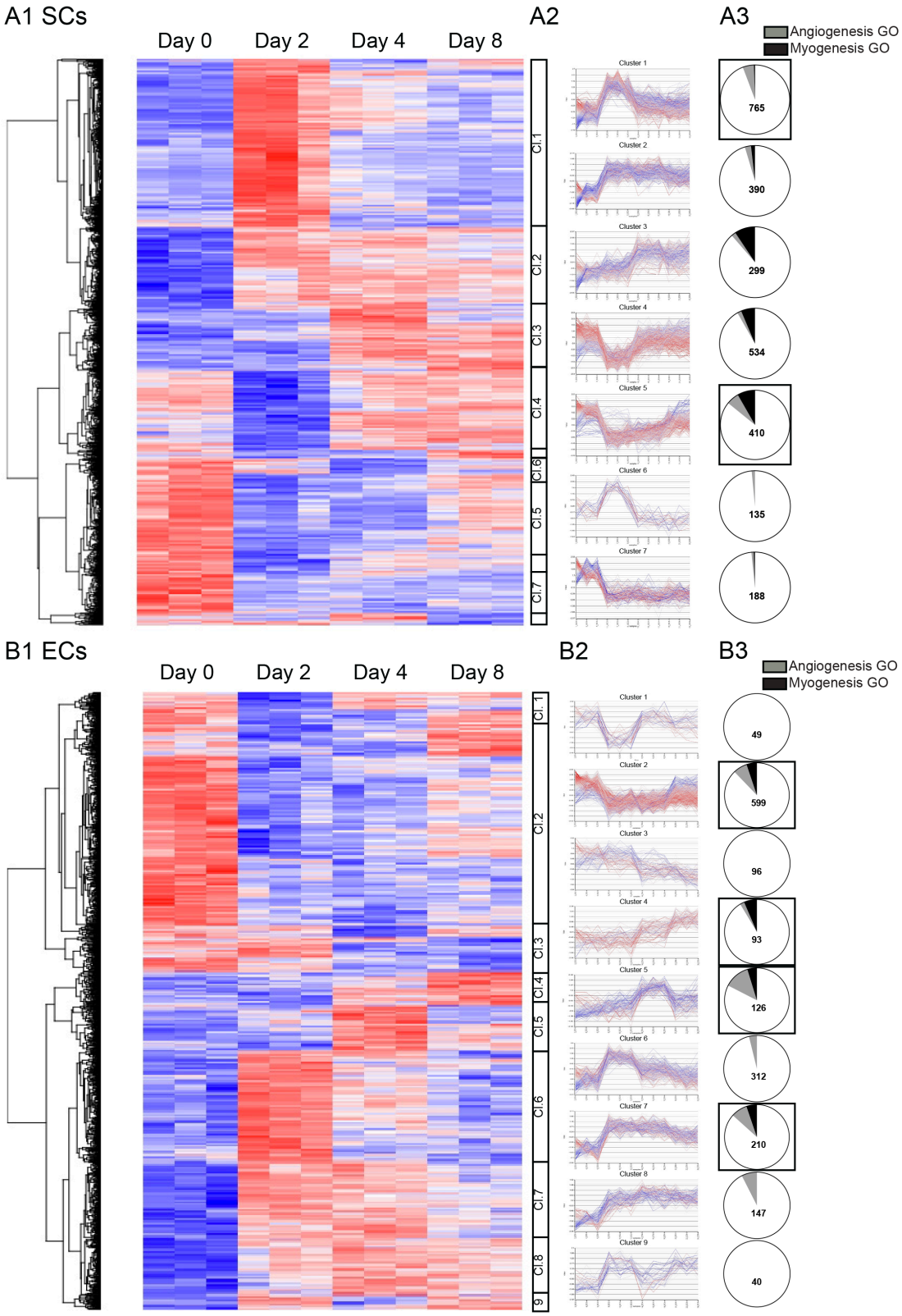

Figure S2, related to Fig.4. Molecular profiling of sorted ECs and SCs during muscle regeneration. SCs (A) and ECs (B) were isolated at different time points during skeletal muscle regeneration (days 0, 2, 4, 8). mRNAs were prepared and processed for Affymetrix-based analysis. (A1, B1) Clustering of genes expressed by SCs (A1) and ECs (A2) according to their kinetics of expression during muscle regeneration (A2, B2). (A3, B3) Gene Ontology enrichment was performed on each cluster in order to identify transcripts implicated either in angiogenesis (grey) or myogenesis (black), expressed in % of total genes in each cluster in the pie charts. Results were obtained from 3 independent experiments (see Materials and Methods section for statistical analysis). See also Figures 4, 5, 7 for the functional analysis.

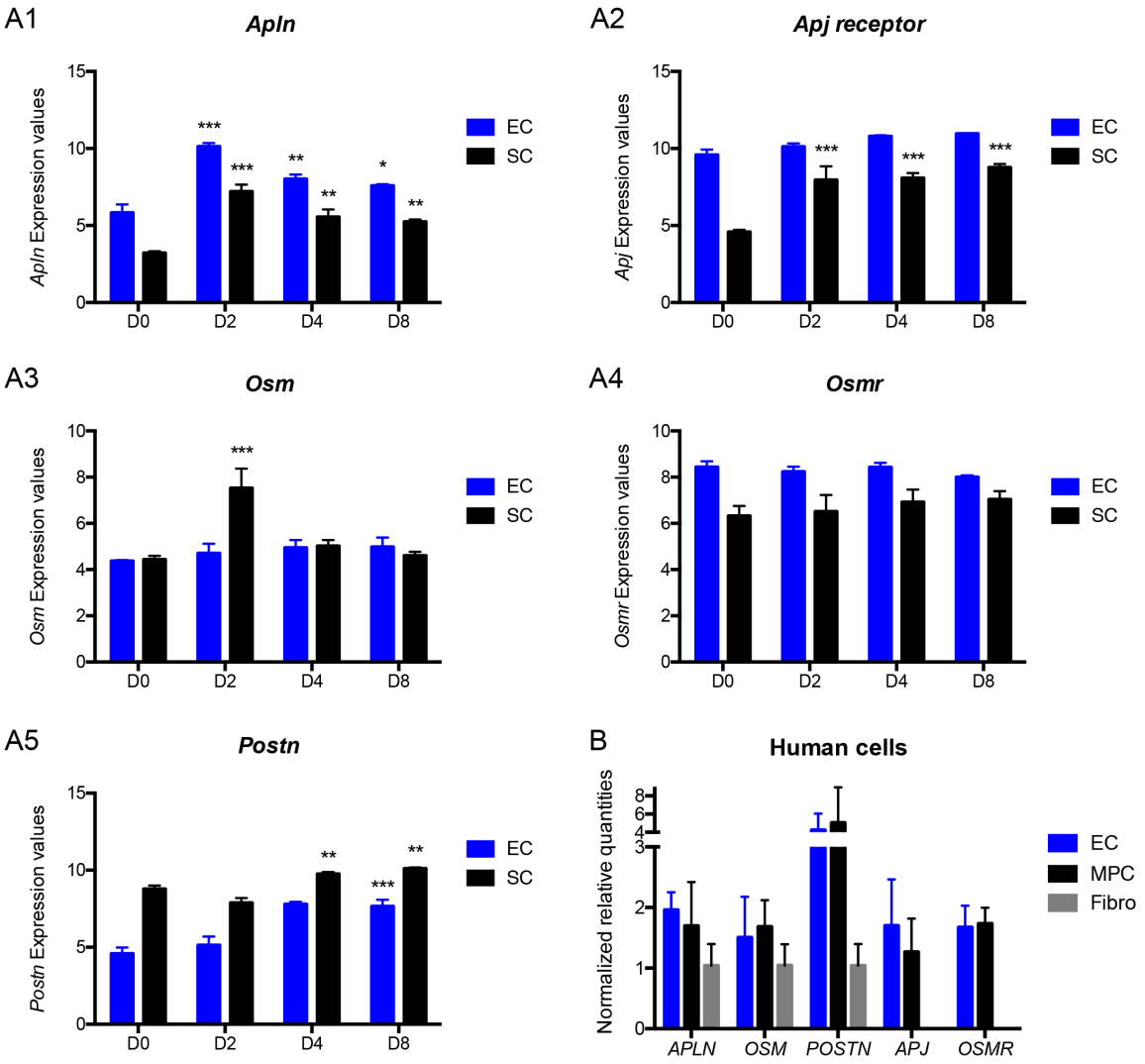

Figure S3, related to Fig.5. mRNA expression of *Apln*, *Osm* and *Postn* in murine and human cells. (A) Expression values from the transcriptomic analysis of *Apln* (A1), *Apjr* (A2), *Osm* (A3) *Osmr* (A4) and *Postn* (A5) in ECs (blue bars) and SCs (black bars) at day 0 or 2, 4 and 8 days post-injury. (B) mRNA expression of the same genes in HUVEC (blue bars), human MPCs (black bars) and Human Normal Dermal Fibroblasts (gray bars) growing *in vitro*. Results are means ± SEM of 3 independent experiments. Mann-Whitney test was performed *versus* D0 *=p<0.05; **=p<0.01; ***=p<0.001. See also Figures 4, 5, 7 for the functional analysis.

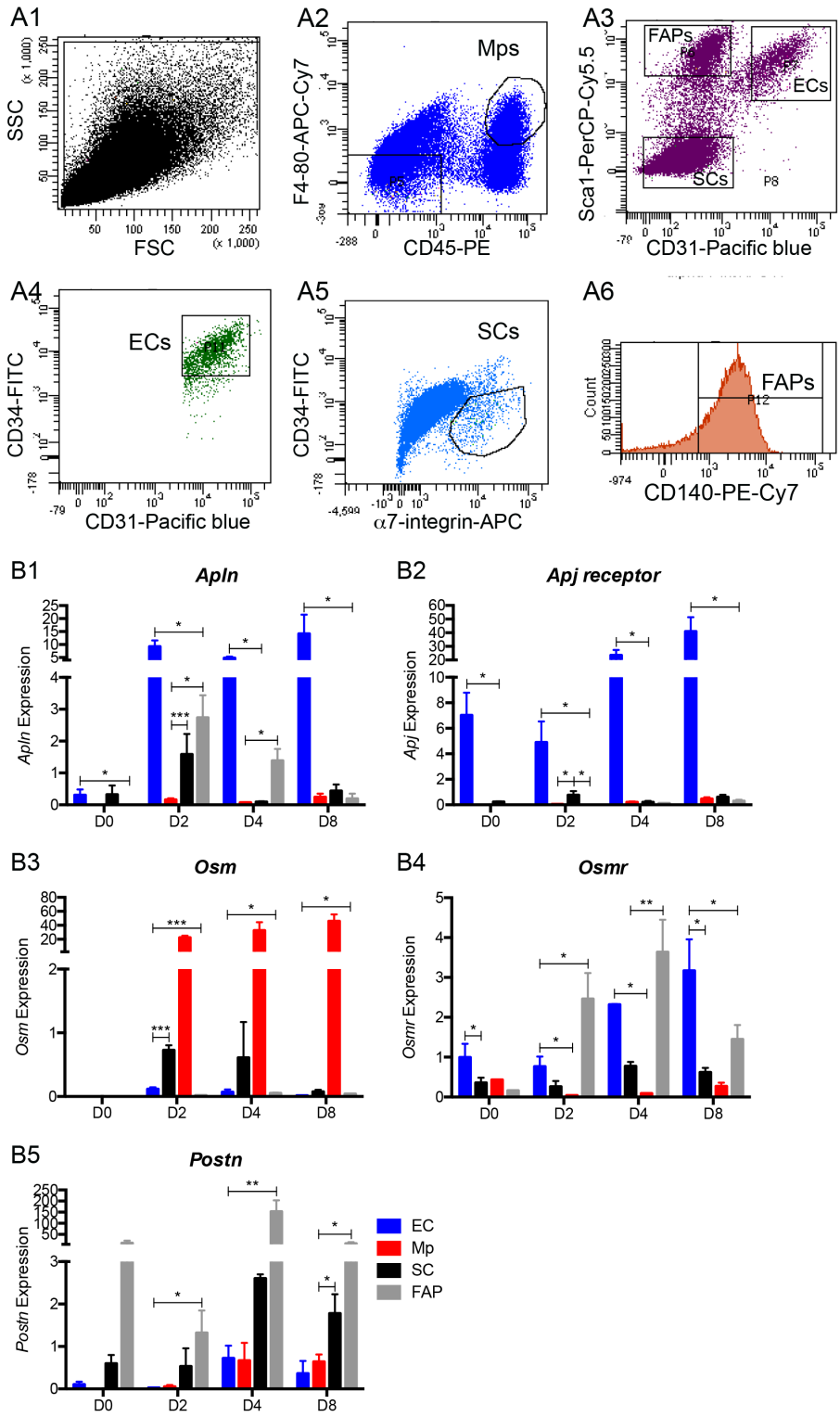

Figure S4, related to Fig.6. EC, SC, Macrophage and FAP isolation from mouse *Tibialis anterior* muscle. At Day 0 and 2, 4 and 8 days after cardiotoxin-induced damage, ECs, SCs, Macrophages (Mps) and Fibro-Adipogenic Precursor cells (FAPs) were FACS-sorted and analyzed for the expression of *Apln*, *Apjr*, *Osm*, *Osmr*, *Postn*. (A) Gating strategy: (A1) Total cell population. (A2) Mps were sorted as CD45+, F4/80+. (A3) Among CD45- F4/80- cells gated in A2, FAPs, SCs and ECs were sorted using Sca1 and CD31 labelings: (A4) Sca1+ CD31+ ECs in A3 were 100% CD34+; (A5) Sca1-, CD31- cells in A3 were further sorted as CD34lo α7 integrin+ SCs; (A6) Sca1+ CD31- FAPs in A3 were almost 100% CD140+ (PDGFRα). (B) RT-qPCR for (B1) *Apln*, (B2) *Apjr*, (B3) *Osm*, (B4) *Osmr*, (B5) *Postn* was performed on the 4 isolated cell populations. Results are means ± SEM of 3 independent experiments. Student t test was performed *versus* the other cell types *=p<0.05; **=p<0.01; ***=p<0.001 (see bars). See also Figure 6 for the functional analysis.

Table S1, related to Fig.S1, S2. List of factors secreted by ECs and SCs during skeletal muscle regeneration
See excel file

Table S2. Oligonucleotide primers used for qPCR, Related to Fig.S3, S4

Human primer	Forward sequence	Reverse sequence
CycloA	5'-GTCAACCCCACCGTGTTCTT-3'	5'-CTGCTGTCTTTGGGACCTTGT-3'
APLN	5'-ATAAGGGACCCATGCCTTTC-3'	5'-CCTCCAGAGAAGCAGACCAA-3'
APJ/APLNR	5'-ACTTCTTCATCGCCCAAACC-3'	5'-ATCCAGCACAGGGCAAAG-3'
OSM	5'-ACAGAGGACGCTGCTCAGTC-3'	5'-GGTGTCCTGCATGAGATCTGT-3'
OSMR	5'-GCAAGTCAAGGAAATGTCAGTG-3'	5'-CCCCAAGGCAGTGTCCGTCC-3'
POSTN	5'-CCATCTGTGGACAGAAAACG-3'	5'-CATGGTCAATGGGCAAAAC-3'

Murine primer	Forward sequence	Reverse sequence
Rpl13	5'-CTCTGGCCTTTTCCTTTTTG-3'	5'-CCGAAGAAGGGAGACAGTTC-3'
APLN	5'-GGAATTCGGGACCATGAATCTGAGGCTCTG-3'	5'-ACTTGGCGAGCCCTTCAATC-3'
APJ/APLNR	5'-GTGGCCACAGCAGTCTTATG-3'	5'-GAACACCATGACAGGCACAG-3'
OSM	5'-TGCTCCAACTCTTCCTCTCAG-3'	5'-CAGGTTTTGGAGGCGGATA-3'
OSMR	5'-CCAAAAAGAGTTCAGCACACC-3'	5'-CCGACCACACTTGTCTCCAT-3'
POSTN	5'-GAACCAAAAATTAAAGTCATTCAAGG-3'	5'-GGATCTTCGTCATTGCAGGT-3'

Supplemental Experimental Procedures

Human MPC Culture. Human MPCs were isolated from normal adult skeletal muscle sample according to the French legislation (protocol registered at the Agence de la Biomedecine #DC-2009-944), as previously described (Saclier et al., 2013) in HAMF12 medium (Gibco) containing 15% Fetal Bovine Serum (FBS). Conditioned medium was recovered after 24h culture in advanced RPMI 1640 medium (Gibco) containing 0.5% FBS. To obtain differentiated myocytes, MPCs were cultured for 72 h at low density (3000 cells/cm^2) in HAMF12 medium containing 5% FBS. To obtain myotubes, myocytes were seeded at high density (15000 cells/cm^2) in differentiating medium DMEM (Gibco) supplemented with Insulin and transferrin (50 mg/ml) and cultured for 72 h. In some experiments, MPCs were transduced with RFP lentivirus. The lentiviral vector particles were produced by transient transfection of the packaging construct (HIV-1 psPAX2), a minimal genome (HIV-1 SPARQ QM512-B2 from SBI) bearing the expression cassette encoding the RFP-puromycin fusion and the plasmid encoding the VSV-G-envelope expressing plasmid pMDG2 (DNA ratio 8:8:4 µg) into 293T cells (3.5 x 10^6 cells plated 1 day before transfection in 100-mm dishes) by the calcium phosphate method. Viral particles were 100X concentrated on 25% sucrose cushion and homogenized viral particles were normalized by an exogenous reverse transcriptase assay and titrated on target cellular models as in (Alais et al., 2012).

HUVEC Culture. HUVEC were obtained from Promocell and cultured in ECGM-2 complete medium (Promocell). They were transduced with GFP lentivirus and purified by cell sorting on GFP labeling (Aria III, BD Biosciences). Conditioned medium was recovered after 24h culture in advanced RPMI 1640 medium containing 0.5% FBS.

Migration assay. Migration was performed using two chambers Ibidi inserts (Ibidi GmbH). Each chamber was filled with 4500 MPCs or HUVEC for 8-12h in growth medium. Silicone walls were removed and cells were cultured in advanced RPMI medium 1640 containing 0.5% FBS. The gap between the two cell types was imaged at 0 and 24 h. The distance covered by each individual cell was measured using Image J software.

Proliferation assay. MPCs or HUVEC were seeded at 5000 cells/cm^2 in multi-well plates. HUVEC- and MPC-conditioned medium was added and cells were further cultured for 24 h. In some experiments, cells were cultured in the presence of recombinant proteins (hPOSTN 0.1, 0.5, 5, 10 µg/ml, hOSM 5, 10, 50, 100 ng/ml, APLN13 1, 10, 100, 1000 nM, Biotechne) for 24 h in HAMF12 medium containing 5% FBS. Ki67 immunolabeling or EdU staining was then performed.

Myogenic differentiation. MPCs were seeded at 5000 cells/cm^2 in multi-well plates. HUVEC-conditioned medium was added and cells were further cultured for 72h. Myogenin immunolabeling (sc-12732 Santa Cruz) was performed. In some experiments, cells were cultured in the presence of recombinant proteins (hPOSTN 0.1, 0.5, 5, 10 µg/ml, hOSM 5, 10, 50, 100 or 200 ng/ml, APLN13 1, 10, 100, 1000 nM, Biotechne) for 72 h in HAMF12 medium containing 5% FBS.

Myogenic fusion. Human MPCs were cultured for 3 days in HAMF12 medium containing 5% FBS to differentiate into myocytes. They were then seeded at 50000 cells/cm^2 in 96-well plates. HUVEC-conditioned medium was added and cells were further cultured for 72 h. In some experiments, cells were cultured in the presence of recombinant proteins (as above) for 72 h in HAMF12 medium containing 5% FBS. Desmin immunolabeling (ab32362 abcam) was performed. Fusion index was the number of nuclei in myotubes divided by the total number of nuclei.

3D *in vitro* angiogenesis assay. HUVEC-GFP were combined with the cytodex beads (Millipore) at a ratio of 400 cells/bead for 4 h at 37°C with occasional stirring. The HUVEC-coated cytodex beads were cultured overnight in a T75 flask in ECGM-2 medium, and then combined in the pre-gel solution at a concentration of 250 beads/ml. Fibrinogen type I (Sigma) was diluted to 2.5 mg/ml and supplemented with aprotinin (1/500 Sigma). MPCs, myocytes or myotubes were added to the pre-gel at various concentrations (50000 to 250000 cells/ml). In some experiments, ECs or MPCs were seeded alone and IgG, blocking antibodies or inhibitors (Biotechne) were added as follows: anti-OSM antibodies (50 µg/ml), ML221 (16 µM), anti-POSTN antibodies (40 µg/ml). Fibrin gel formation was initiated by adding 10 U/ml of thrombin (Sigma). The gels were allowed to stand for 5 min at room temperature, and then were incubated at 37°C for 15 min. In some experiments, human dermal fibroblasts (NHDF, Promocell) or MPCs or macrophages (the latter being previously activated with IL-4 or with IL-10 and Dexamethasone as described in (Saclier et al., 2013)), were seeded on top of the gel (60000 cells). The cells were cultured in EndoGro media (Millipore) up to 6 days. The medium was refreshed every 2 days. Micrographs captured the tube formation, and quantification was completed using Image J. Sprouts were measured as tubes originating from the cytodex bead. Each sprout length was calculated, as well as the presence of lumen in the sprout. For each condition, a minimum of 100 sprouts was analyzed.

Mice. Adult male C57Bl/6 mice were bred and used in compliance with French and European regulations. Principal investigators are licensed for these experiments and the protocols were approved by local Animal Care and Use Committee and the French Ministery of Agriculture.

***In vivo* muscle regeneration.** Muscle injury was caused by intramuscular injection of cardiotoxin (12µM, 50µl) in the *Tibialis Anterior* muscle, as previously described (Mounier et al., 2013). Muscles were harvested 2,4,8

days post-injury. Muscle fascia were removed, then muscles were either dissociated (for cell sorting) or snap frozen in nitrogen-chilled isopentane and kept at -80°C until use (for histological analysis). In some experiments, blocking antibodies or inhibitors (Biotechne) were injected intramuscularly as follows: blocking anti-OSM antibodies (5 µg) or ML221 (Apelin receptor APJ antagonist, 5 µg) were injected i.m. at days 2 and 3 post-injury (controls included the injection of same volume of PBS or PBS containing 2.6% DMSO). Blocking anti-POSTN antibodies (5 µg) were injected at days 3 and 4 post-injury. Muscles were collected for histological analysis at day 8.

Histology analysis. 7 µm-thick cryosections were prepared for hematoxylin-eosin staining or for immunolabeling. Muscles cryosections were treated with anti- laminin (L9393 sigma), CD31 (550274 Pharmingen), Ki67 (ab15580 abcam), Pax7 (Developmental Studies Hybridoma Bank, DSHB), Myogenin (SC-576 Santa Cruz Biotechnology), MyH3 (SC-53091 Santa Cruz Biotechnology) antibodies revealed with conjugated secondary antibodies (Jackson Immunoresearch Inc). Two-dimensional analysis was performed to evaluate the cross-section area of myofibers, the number of nuclei per fiber, the number of myogenin^{pos} cells, the number of Myh3^{pos} fibers, the number of SCs (Pax7^{pos}) per fiber, and the number of capillaries per fiber using ImageJ software. At least 300 fibers were considered for each muscle.

***In vivo* angiogenesis assay.** Primary murine MPCs were cultured in DMEM/F12 (Gibco) medium containing 20% FBS (Gibco) and 2% Ultroser G as previously described (Mounier et al., 2013). NIH3T3 cells were cultured in DMEM containing 15% FBS. Cells ($1x10^6$ cells/ml) were embedded in cold Matrigel® (BD Biosciences) and 500 µl of the mix were injected subcutaneously in 4-6-week-old male C57Bl/6 mice. In some experiments, recombinant proteins were added: mPOSTN 5 µg/ml, mOSM 50 ng/ml or APLN13 10 nM (Biotechne). After 21 days, mice were euthanized and plugs were recovered and fixed in JB fixative (zinc acetate 0.5%, zinc chloride 0.05%, and calcium acetate 0.05% in Tris buffer at pH 7.0) for 48 h and then embedded in low–melting point paraffin (Poly Ethylene Glycol Distearate, Sigma). 5 µm thick paraffin sections were deparaffinized in absolute ethanol, air dried, and used for H&E staining and immunolabeling. Sections were treated with anti- CD31 (ab28364 abcam), desmin (ab6322 abcam) and α-SMA (ab5694 abcam) antibodies and revealed with conjugated secondary antibodies (Jackson Immunoresearch Inc). Blood vessel infiltration into the plug and desmin-expressing cells (MPCs) were quantified on the totality of a plug section, by evaluating the vessel and MPC staining area using ImageJ software. Functional angiogenesis inside the plug was evaluated as the amount of hemoglobin using the Drabkin's reagent (Sigma) following the manufacturer's instructions.

Cell sorting from regenerating muscle. Single cell suspensions were obtained from muscles by enzymatic digestion (Collagenase B 10 mg/ml and Dispase 2 2.4U/ml, Roche Diagnostics). ECs, SCs, macrophages and FAPs were isolated using anti-CD45 PE, F4-80 APC-Cy7, CD34-FITC, Sca1-eFluor 605 or PerCP-Cy5.5, ✔7-integrin-APC, CD31-eFluor 450 and PDGFRα (CD140a) PE-Cy7 antibodies and their respective isotype controls (all from eBioscience except alpha7-integrin from Ablabs, British University of Columbia). Aria III (BD Biosciences) was used for cell sorting and LSRFortessa for cell analysis (BD Biosciences). All analyses and quantifications were performed using FACSDIVA software (BD Biosciences). To control cell purity, sorted MPCs and ECs were cytospined and labelled with primary antibodies against Pax7 (DSHB), VE-cad (sc-6458 Santa Cruz) and CD31 (ab28364 Abcam).

Transcriptomic analysis. Total RNAs were extracted from sorted ECs or MPCs using RNeasy Mini Kit (Qiagen). RNA integrity was checked on Agilent Bioanalyser 2100, RNA samples with >9.0 RIN value were used. Global expression data were obtained using Affymetrix GeneChip Mouse Gene 2.0 ST arrays. The microarray data are publicly available (Deposition in GEO currently in progress). Data were RMA normalized with R/Bioconductor. Data were first controlled and analyzed in an unsupervised way by PCA and a one-way ANOVA was applied to extract DEGs using PartekGS© software. Genes were selected on the global p value <0.01. A cluster analysis was then applied on selection by hierarchical clustering (Pearson for similarity and average for clustering) to find correlate genes. Enrichment analysis of each cluster was analyzed with DAVID software (https://david.ncifcrf.gov/) (Huang da et al., 2009). Pathway Studio© software (Elsevier BV) was used to identify extracellular effectors synthetized by ECs and MPCs that triggered enrichment in "myogenesis" and "angiogenesis" GOs in MPCs and ECs, respectively (strategy is presented in Figure S1J). A list of genes expressed by both ECs and MPCs was finalized (Table S1).

qRT-PCR. mRNAs of sorted or cultured cells were extracted using RNeasy Mini Kit (Qiagen). One µg of total RNA was reverse transcribed into first-strand cDNA using Superscript II Reverse Transcriptase (Life technologies). Quantitative PCR was carried out on StepOne Plus RealTime PCR system (Applied Biosystems). Reaction mixtures had a final volume of 20 µl, consisting of 1 µl of cDNA, 10 µl of Sybr Green Master (Roche) and 10 µM of primers, listed in Table S2. After initial denaturation, amplification was performed at 95°C (10 s), 60°C (5 s), 72°C (10 s) for 45 cycles. Calculation of relative expression was determined by the StepOnePlus software (Applied Biosystems) and fold change was normalized to CycloA housekeeping gene for human cells and RPL13 for murine cells.

Microscope image acquisition. Samples were observed using a Zeiss Axio Observer.Z1 microscope, and recorded at 22-24°C with a Photometrix CoolSNAP HQ2 camera using Metaview software. Magnification was

x20 for histological experiments; x20 for 2D *in vitro* experiments and x10 for 3D experiments. Mounting medium was FluoroMount-G (Interchim). Secondary antibodies were from Jackson Immunoresearch Inc and coupled with FITC, Cy3 or Cy5 fluorochromes. Nuclei were labeled with Hoechst. Pictures were analyzed using ImageJ software using manual counting.

Statistics. All experiments were performed in at least 3 independent experiments, *i.e.* different primary cultures or different animals. The exact number of experiments and statistical significance are given in the figure legends. Results are expressed as mean ± SEM. Means were compared using Mann Whitney or two-way ANOVA and Sidak post-tests.

Supplemental References

Alais, S., Soto-Rifo, R., Balter, V., Gruffat, H., Manet, E., Schaeffer, L., Darlix, J.L., Cimarelli, A., Raposo, G., Ohlmann, T.*, et al.* (2012). Functional mechanisms of the cellular prion protein (PrP(C)) associated anti-HIV-1 properties. Cell Mol Life Sci CMLS *69*, 1331-1352.

Huang da, W., Sherman, B.T., and Lempicki, R.A. (2009). Bioinformatics enrichment tools: paths toward the comprehensive functional analysis of large gene lists. Nucleic Acid Res *37*, 1-13.